Quaternary normal faulting in southeastern Sicily (Italy): a seismic source for the 1693 large earthquake

Marcello Bianca,[1] Carmelo Monaco,[1] Luigi Tortorici[1] and Licio Cernobori[2,3]

[1] *Istituto di Geologia e Geofisica, Università di Catania, Corso Italia 55, 95129 Catania, Italy. E-mail: tortoric@mbox.unict.it*
[2] *Dipartimento Ingegneria Navale per il Mare e per l'Ambiente, Università di Trieste, Via Valerio 10, 34127 Trieste, Italy*
[3] *Osservatorio Geofisico Sperimentale, Trieste, Italy. E-mail: lcernobori@ogs.trieste.it*

SUMMARY
We present geological and morphological data, combined with an analysis of seismic reflection lines across the Ionian o shore zone and information on historical earthquakes, in order to yield new constraints on active faulting in southeastern Sicily. This region, one of the most seismically active of the Mediterranean, is a ected by WNW–ESE regional extension producing normal faulting of the southern edge of the Siculo–Calabrian rift zone. Our data describe two systems of Quaternary normal faults, characterized by di erent ages and related to distinct tectonic processes. The older NW–SE-trending normal fault segments developed up to ≈ 400 kyr ago and, striking perpendicular to the main front of the Maghrebian thrust belt, bound the small basins occurring along the eastern coast of the Hyblean Plateau. The younger fault system is represented by prominent NNW–SSE-trending normal fault segments and extends along the Ionian o shore zone following the NE–SW-trending Avola and Rosolini–Ispica normal faults. These faults are characterized by vertical slip rates of 0.7–3.3 mm yr^{-1} and might be associated with the large seismic events of January 1693. We suggest that the main shock of the January 1693 earthquakes ($M \sim 7$) could be related to a 45 km long normal fault with a right-lateral component of motion. A long-term net slip rate of about 3.7 mm yr^{-1} is calculated, and a recurrence interval of about 550 ± 50 yr is proposed for large events similar to that of January 1693.

Key words: earthquakes, normal faulting, seismic reflection, seismotectonics, southern Italy.

1 INTRODUCTION

Southeastern Sicily is one of the most seismically active areas along the boundary between the African and Eurasian plates in the central Mediterranean. Several historical seismic events, such as the 1169 and 1693 earthquakes, reached MCS intensities of XI ($M \sim 7$) (Fig. 1). This area, mostly represented by the Hyblean Plateau, is bordered to the east by active normal faults that contribute to a continuous extensional deformation from the Ionian coasts of Sicily to northern Calabria (Siculo-Calabrian rift zone; Monaco *et al.* 1997). Normal faults are due to a ESE–WNW regional extension (Tortorici *et al.* 1995; Monaco *et al.* 1997) which is marked by a high level of crustal seismicity producing earthquakes with normal focal mechanisms (Cello *et al.* 1982; Gasparini *et al.* 1982) and intensities of up to XI–XII MCS and $M \sim 7$ (Baratta 1901; Postpischl 1985a; Boschi *et al.* 1995a).

The Hyblean Plateau is characterized by a continental crust overlain by thick Mesozoic to Quaternary carbonate sequences and represents the emerged foreland of the Neogene–Quaternary Maghrebian thrust belt (Fig. 1). To the NW, the flexured border of this domain, during Upper Pliocene–Lower Pleistocene times, was downfaulted beneath the frontal part of the Maghrebian thrust belt (Cogan *et al.* 1989; Grasso & Pedley 1990) in response to the NNW–SSE-orientated convergence between Africa and Europe (Dewey *et al.* 1989). To the east, the Hyblean Plateau is a ected by a network of normal faults which bound a number of Plio–Pleistocene basins and have been related to the activity of the Malta Escarpment (Grasso & Lentini 1982; Grasso *et al.* 1990). This forms a long-lived weakness belt representing the Mesozoic boundary separating this continental domain from the oceanic crust of the Ionian basin (Scandone *et al.* 1981; Makris *et al.* 1986).

The Quaternary evolution of this geological domain has been mostly dominated by normal faulting, which has controlled the landscape morphology and both the onshore and o shore basin development. The vertical component of deformation a ecting this region has been recorded by several
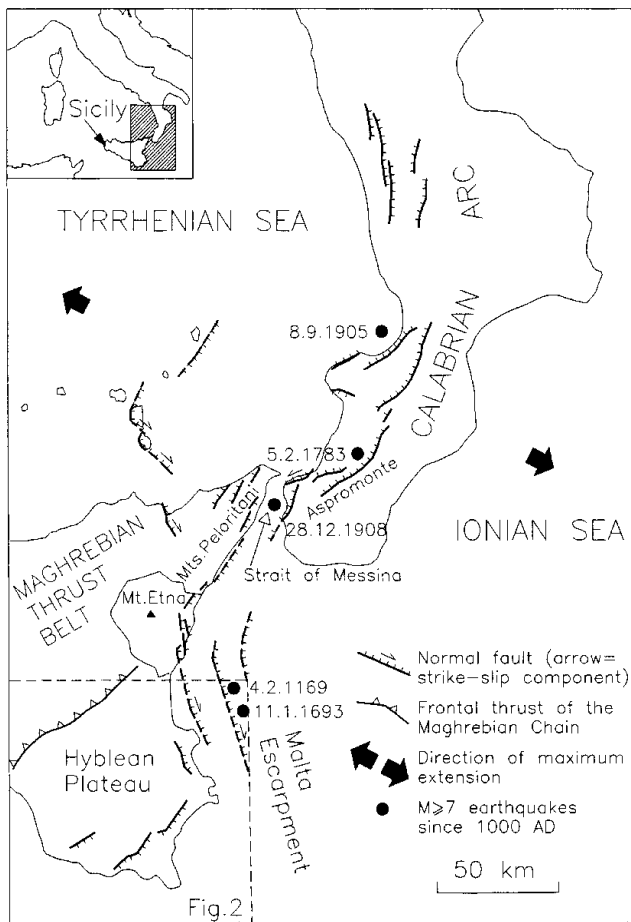
Figure 1. Seismotectonic map of eastern Sicily and the Calabrian arc.

with seismological data have been carried out, the large 1169 and 1693 earthquakes have still not been related to specific seismic sources. Active faults responsible for these seismic events have been located either onland, along the northern boundary of the Hyblean Plateau (Mulargia *et al.* 1985; D'Addezio & Valensise 1993; Boschi *et al.* 1995b), or o shore along the Malta Escarpment (Carbone *et al.* 1982; Postpischl 1985b; Piatanesi & Tinti 1998).

The aim of this study is to define the role of the major Quaternary fault segments and to test the possible relationships between faults and earthquakes. The integration of geological and geophysical data of the eastern part of the Hyblean Plateau, including seismic profiles across the Ionian o shore area, and a detailed analysis of historical documents describing the 1693 earthquakes, provide new constraints on the origin of the seismic activity as associated with the major Quaternary fault segments of this area.

2 LARGE-SCALE QUATERNARY DEFORMATION OF THE EASTERN HYBLEAN PLATEAU

Recent geological and morphological features of the eastern margin of the Hyblean Plateau result from the extensional tectonics that a ected this region during the Quaternary. In the northeastern part (Fig. 2), the Quaternary basins of Augusta-Siracusa and Floridia correspond to tectonic depressions separated by uplifted ridges (e.g. the Mt Climiti ridge) controlled by impressive normal fault segments such as the Mt Climiti fault (CF). To the south, Quaternary normal faulting generated the Avola fault (AF) and Rosolini–Ispica fault system (RIFS) (Monaco & Tortorici 1995). This region also shows several strands of marine terraces that developed on both the tectonic depressions and ridges, indicating that it has represented, at least since the Middle Pleistocene, the uplifted block of a large normal fault system located in the Ionian o shore area (Hirn *et al.* 1997).

Marine terraces represent useful markers for evaluating uplift movements occurring in tectonically active regions. Terraces, which are represented by wave-cut surfaces and/or thin depositional platforms, develop during both the marine high and low stands. The inner edge of the terraced surfaces and the alignments of marine caves and notches carved in the coastal cli s represent a remarkable record of the palaeoshorelines formed at sea level during a marine stillstand.

The Quaternary period was marked by cyclic glacio-eustatic global sea level changes which are well recorded by the curve of the oxygen isotope timescale (OIT). Based on the variations of $\delta^{18}O$, various workers (e.g. Imbrie *et al.* 1984; Martinson *et al.* 1987; Bassinot *et al.* 1994) characterize peaks corresponding to distinct marine high and low stands (Fig. 3a). The absolute sea level calculated for the peaks related to the last 400 kyr of the OIT curve (Shackleton & Opdyke 1973; Chappell & Shackleton 1986; Merritts & Bull 1989; Chappell *et al.* 1996) underwent important variations, reaching about 130 m below the present sea level during the last glacial climax, and 6 m above the present sea level during the Tyrrhenian interglacial period (Fig. 3b). This implies that strands of terraces and palaeoshorelines are visible only in uplifted regions, with the number of orders rising with increasing uplift rate. By combining ages and elevations of palaeoshorelines with OIT stages
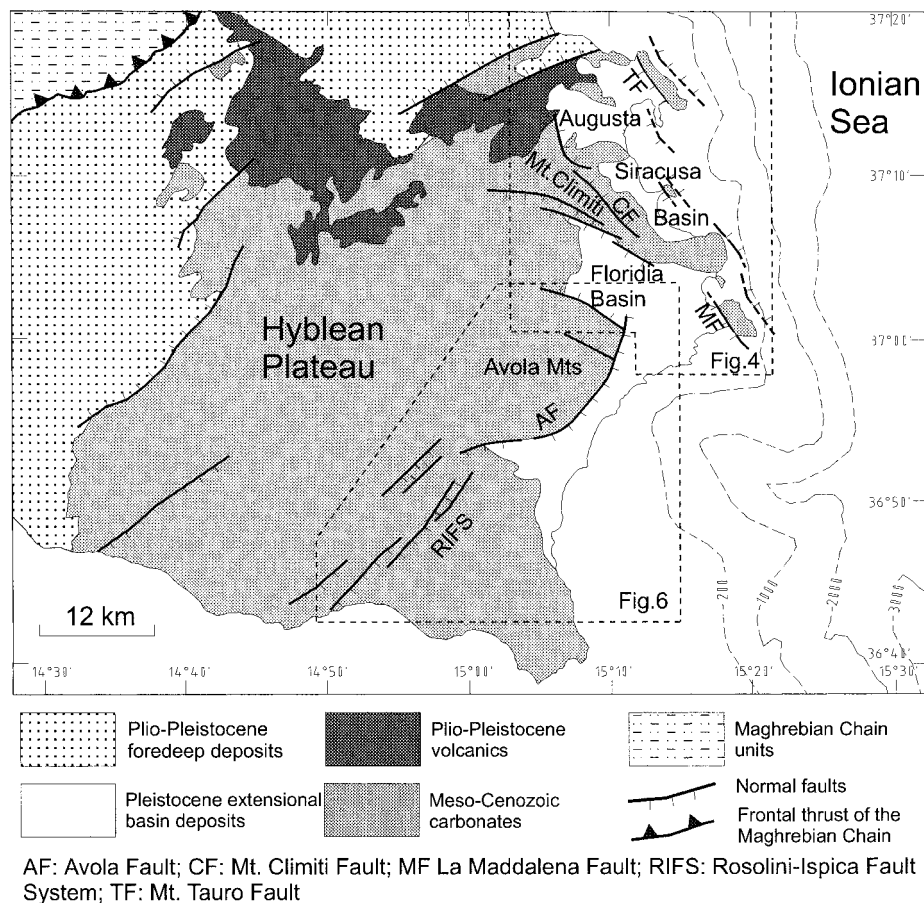
orders of Middle–Upper Quaternary marine terraces and palaeo-strandlines which, as reported in studies by Accordi (1963), Di Grande & Raimondo (1982) and Bordonaro *et al.* (1984), occur extensively along the eastern part of the Hyblean Plateau. Despite the occurrence of this well developed flight of terraces, which should be associated with high rates of uplift, a very low uplift rate (about 0.2 mm yr^{-1}) is reported by Cosentino & Gliozzi (1988) for this region. This value, also quoted in Bordoni & Valensise (1998), contradicts the detailed stratigraphic observations (Accordi *et al.* 1959; Accordi 1963; Di Grande & Raimondo 1982; Bordonaro *et al.* 1984; Malatesta 1985; Di Grande & Neri 1988) and the absolute dating (Belluomini & Bada 1985; Bada *et al.* 1991; Rhodes 1996) carried out on deposits belonging to distinct orders of terraces, which imply higher values of uplift rates. Moreover, this conflict is enhanced by the regional tectonic framework that characterizes the Ionian coast of Sicily. The eastern part of the Hyblean Plateau is, in fact, located on the footwall of the large Quaternary normal fault system that northward (Fig. 1) bounds the uplifted blocks of the Peloritani mountain range and the Aspromonte massif (Tortorici *et al.* 1995; Monaco *et al.* 1997), which are characterized by cumulative (both regional and fault-related) uplift rates higher than 1 mm yr^{-1} (Westaway 1993; Stewart *et al.* 1997). The uncertainties over both the overall distribution of marine terraces and the rates of recent vertical movements have given rise to poorly constrained seismotectonic schemes of the area. Although studies combining tectonic observations

Figure 2. Structural sketch map of southeastern Sicily. For location see Fig. 1.

of high sea level stands and absolute sea level variations it is thus possible to evaluate the uplift rates of rising regions accurately (Westaway 1993; Armijo *et al.* 1996; Bosi *et al.* 1996).

2.1 Marine terraces

In order to evaluate the Quaternary uplift of the Hyblean Plateau, we detailed the distribution of marine terraces along the Ionian coast (Table 1 and Fig. 4). The marine terrace surfaces, with their relative inner and outer edges, have been mapped over the whole area using the 1 : 25 000 scale topographic maps of the Istituto Geografico Militare, SPOT satellite images, and 1 : 33 000 and 1 : 10 000 scale aerial photographs. This information was coupled with detailed field observations, which in the most important areas have been traced on the Regione Siciliana 1 : 10 000 scale topographic maps.

2.1.1 Augusta–Siracusa area

The area located between Augusta and Siracusa exhibits several marine terraces with preserved inner edges (Fig. 4). The terraces developed above both the soft sediments infilling the Quaternary depressions (Augusta–Siracusa and Floridia basins) and the Mesozoic–Cenozoic carbonates forming the ridges. Seven main terrace platforms with their inner and outer edges and remnants of two palaeoshorelines have been traced. These data are consistent with the studies of Di Grande &

Raimondo (1982) and Bordonaro *et al.* (1984), although their observations, which are of more restricted areas, are reported in schematic maps lacking topographic information. In order to describe clearly the various orders belonging to the flight of terraces occurring along the Ionian side of the Hyblean Plateau, we have chosen the Belvedere–Mt Climiti ridge as a reference area. In this area, which separates the Augusta–Siracusa basin from the Floridia basin, the individual levels of marine terraces, directly engraved into the calcareous substratum, are clearly recognizable. The terraces have been mapped on the Regione Siciliana 1 : 10 000 scale topographic maps (contour elevation lines of 5 m) with an uncertainty in the elevation of the inner edges of ± 3 m. This uncertainty, which basically depends on erosional and depositional processes following the emergence of the terrace, is, however, negligible when estimating the long-term Quaternary uplift rates involving time span of tens to hundreds of thousands of years. The terraces that we mapped have been named with the ancient Greek toponyms of the Belvedere region and are represented, in order of descending elevation by the Climiti, Eurialo, Epipoli, Tyche, Neapolis, Akradina, and Siracusa levels (Fig. 4).

The Climiti terrace is represented by a few remnants of a deeply eroded wave-cut platform extending on the top of Mt Climiti (Fig. 4). This surface gently dips eastwards and extends at an elevation ranging from 475 to 340 m over a total length of 2.5 km.

Table 1. Age and uplift rate of inner edges of marine terraces and palaeoshorelines occurring in the Augusta, Belvedere and Floridia areas.

Name	Inner edge elevation in diﬀerent areas (m)			OIT stage	Age (kyr)	Sea level correction	uplift rate (mm yr^{-1})		
	Augusta	Belvedere	Floridia				Augusta	Belvedere	Floridia
Siracusa	15	12	8	3.3	60	+28	0.71	0.66	0.60
Akradina	40	32	20	5.1	80	+19	0.73	0.64	0.48
Neapolis	60	53	45	5.3	100	+9	0.69	0.62	0.49
Tyche	105	85	75	5.5	125	−6	0.79	0.63	0.55
Epipoli	140	120	90	7.1	200	+7	0.73	0.63	0.48
Eurialo	160	145	105	7.5	240	+10	0.70	0.64	0.47
Grottone 2	–	180	–	9.1	300	+27	–	0.69	–
Grottone 1	–	220	–	9.3	330	−4	–	0.65	–
Spinagallo	–	270	200	11.3	410	0	–	0.66	0.48
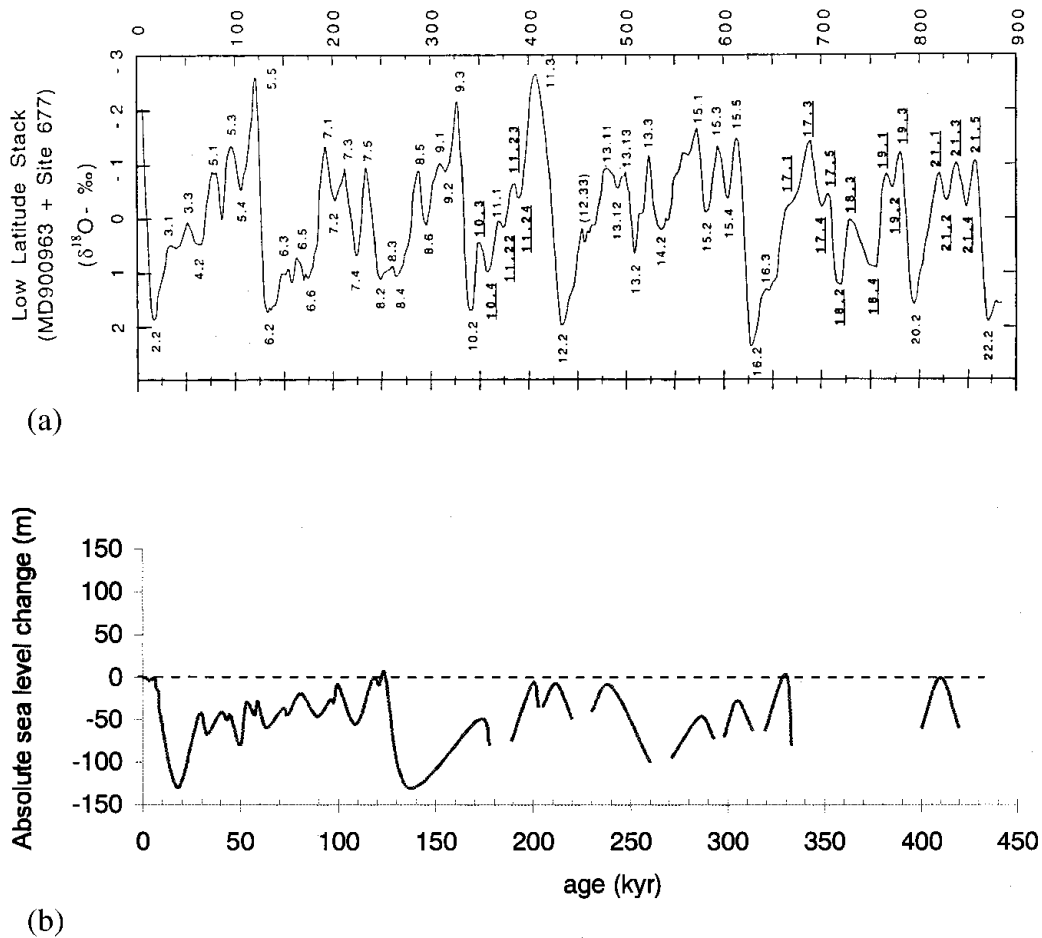
Figure 3. (a) Variations of δ^{18}O during the last 900 kyr and OIT stages proposed by Bassinot *et al.* (1994). (b) Middle Pleistocene–Holocene eustatic curve (data from Shackleton & Opdyke 1973; Chappell & Shackleton 1986; Merritts & Bull 1989; Chappell *et al.* 1996).

Along the eastern escarpment and the southern edge of the Mt Climiti ridge, three main palaeoshorelines are clearly visible. They are characterized by alignments of caves and water-edge notches extending at elevations of 270, 220 and 180 m (Fig. 5a). Between these lines, here called the Spinagallo (see below), Grottone 1 and Grottone 2 lines, respectively, several secondary strandlines are exposed.

The Eurialo terrace mostly comprises a narrow erosional platform cut into the Miocene carbonates in the ridges and into the debris slope that developed at the foot of the Mt Climiti fault scarp (Fig. 4). This platform is bounded landwards by a palaeocoastline, which is located at an elevation of about 145 m in the reference area of Belvedere ridge (Fig. 5a) and extends discontinuously up to the Augusta region where it reaches 160 m in elevation. To the southwest, this line surrounds the southeastern edge of the Mt Climiti ridge thus extending along the western border of the Floridia basin where, reaching an elevation of 105 m, it is covered by alluvial fan deposits. A few metres below, another wave-cut platform, with its inner edge located at an elevation of about 120 m, occurs in the Belvedere ridge (Fig. 5a). This is the Epipoli terrace. Northwestwards, remnants of this platform form a narrow and
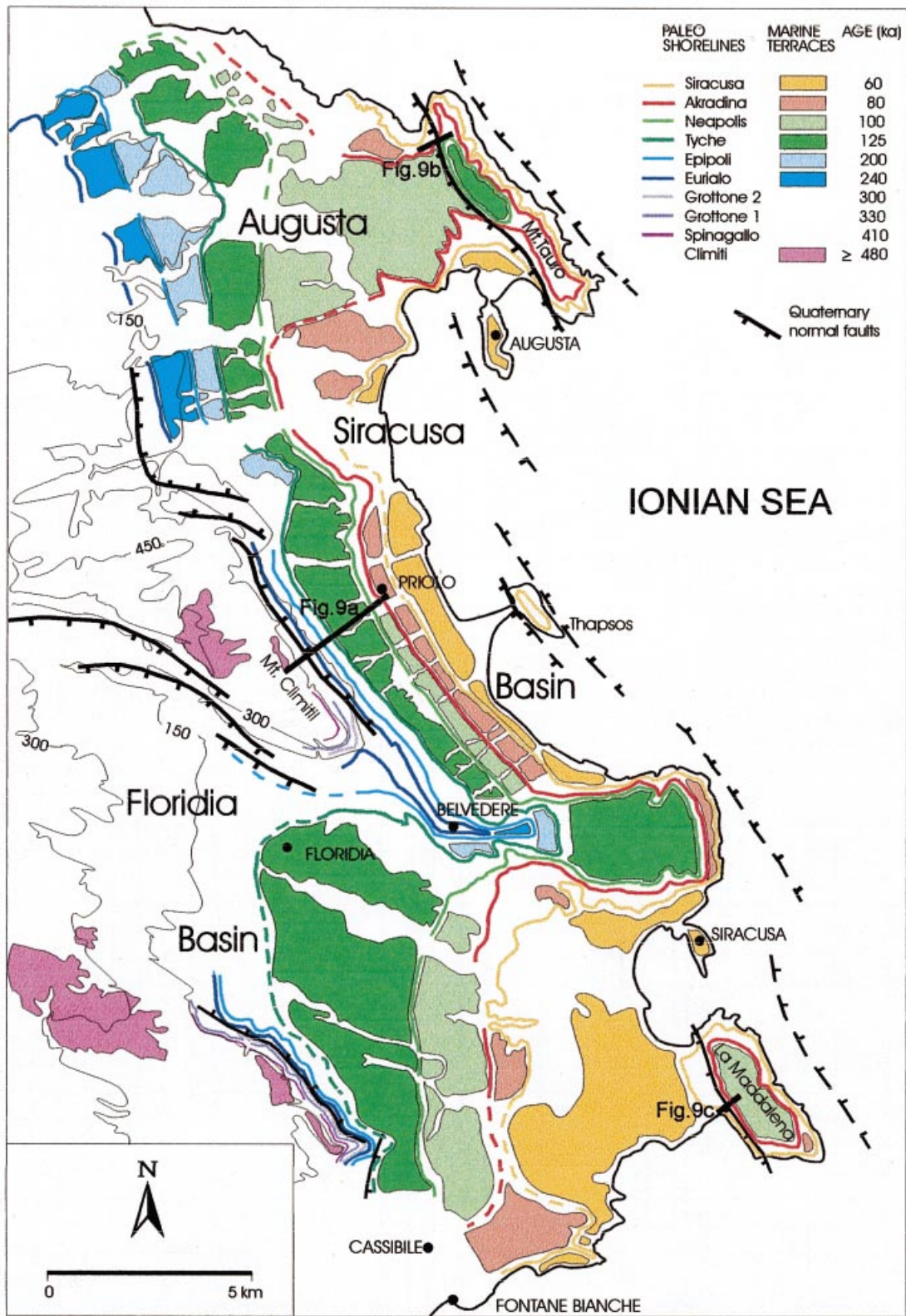
Figure 4. Morphotectonic map of the eastern border of the Hyblean Plateau showing the distribution of marine terraces and palaeoshorelines between Augusta and Siracusa (see Fig. 2 for location). Elevation contour lines are from 1:25 000 IGM topographic maps. The locations of the topographic profiles shown in Fig. 9 are also reported.
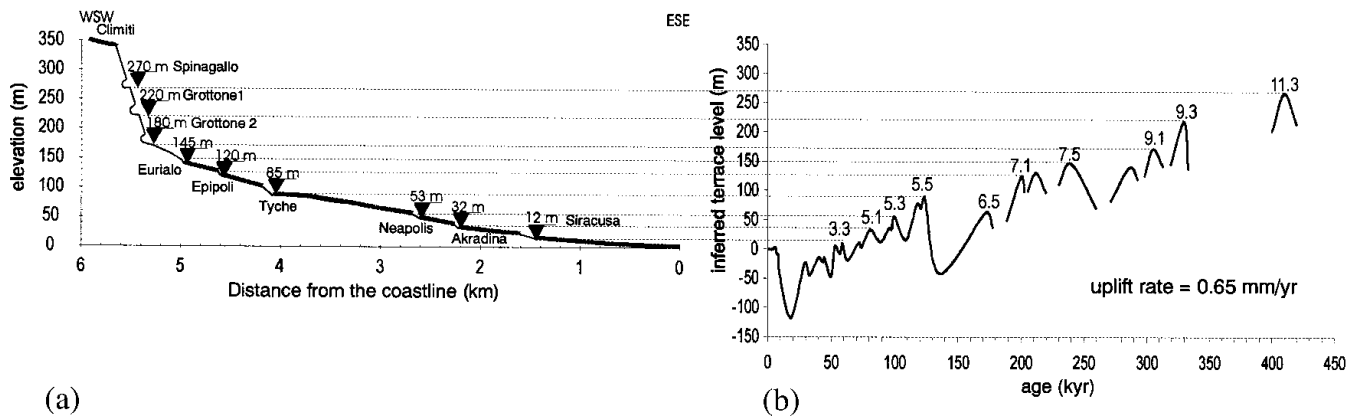
Figure 5. (a) Correlation between the elevations of the inner edges of the marine terraces and palaeoshorelines occurring along a schematic profile traced across the Belvedere ridge area, and (b) the Pleistocene sea level stands corrected for an uplift rate of 0.65 mm yr^{-1}.

discontinuous strip which, by cutting the outer portions of the debris slope developed on the hanging wall of the Mt Climiti fault, extends up to the western border of the Augusta basin (Fig. 4). In the northern part of the Floridia basin, the Epipoli terrace forms a thin depositional platform characterized by cross-bedded beach calcarenites about 10 m thick, which, unconformably overlying the Middle Pleistocene clays, onlap the southwestern flank of the Belvedere ridge (Fig. 4).

The widest terrace in this area is the Tyche terrace. In the Belvedere ridge and along the coastal plain extending between Siracusa and Augusta (Fig. 4), this terrace occurs as an erosional platform, whereas in the Floridia basin it forms a ∼ 10 m thick band of cross-bedded biocalcarenites and sands that rest directly above the Middle Pleistocene clays. Patches of Tyche deposits also occur northwest of the village of Priolo. The inner edge of the Tyche terrace is usually easily recognized across the entire area and it is represented by alignments of well developed shoreline notches carved both in the Epipoli calcarenites in the northern edge of the Floridia basin and in the calcareous substratum of the major headlands, where it is frequently marked by the occurrence of *Lithodomes* holes and encrusting worms. The Tyche palaeocoastline extends at an elevation that decreases from about 105 m in the Augusta area to 75 m in the Floridia basin; it is located at an elevation of 85 m in the Belvedere reference area (Fig. 5a).

The Neapolis terrace is usually represented by a thin depositional platform comprising beach calcarenites. The terrace is exposed across the entire area, usually forming narrow strips except in the Augusta basin where it is represented by a broad calcarenitic platform (Fig. 4). These sediments overlie the Tyche terrace deposits and also unconformably cover the Middle Pleistocene clays in the Augusta basin. Along the northeastern border of the Floridia basin the beach calcarenites of the Neapolis terrace cover remnants of fluvial and lacustrine deposits which were probably deposited during the former sea level lowstand and contain remnants of mammal fauna (Basile & Chilardi 1996). Lens-shaped levels of palaeosoils containing remnants of mammal fauna also occur at the base of this sequence along the western edge of the Augusta basin (Bordonaro *et al.* 1984). The Neapolis terrace in the Maddalena peninsula is found as an erosional platform extending to the top of the headland (Fig. 4). The palaeocoastline that bounds the Neapolis terrace landwards is clearly recognizable and

extends from about 60 m in the northern part of the area to 45 m in the Floridia basin. Immediately south of Belvedere ridge, the inner edge of the Neapolis terrace is located at an elevation of 53 m (Fig. 5a).

The Akradina terrace is mostly represented by a narrow platform related to a palaeoshoreline located, in the reference area, at an elevation of 32 m (Fig. 5a). The inner edge of this terrace, which extends from an elevation of 40 m north of Priolo to 20 m along the southeastern part of the Floridia basin, is well developed across the whole area. It cuts into the Neapolis terrace sediments and, along the major calcareous ridges, into the Miocene deposits. The Akradina coastline surrounds the Mt Tauro and La Maddalena ridges, which, during the relative sea level highstand, represented a peninsula and an island, respectively (Fig. 4). In the Floridia basin, from Priolo to Belvedere and in the northwestern part of the La Maddalena peninsula, the Akradina terrace is depositional, comprising a 1 to 5 m thick cross-bedded biocalcarenite layer (Fig. 4). Along the northern border of the Floridia basin (Basile & Chilardi 1996) and in the northwestern tip of the La Maddalena peninsula (Accordi 1963), the Akradina biocalcarenites lie above lacustrine deposits containing rich fauna comprising remnants of mammals, amphibians, reptiles and birds (Basile & Chilardi 1996). Near Augusta, along the Mt Tauro peninsula (Fig. 4), the Akradina terrace is represented by 2 m thick conglomerates which, in places, contain rare highly damaged, shells of *Strombus bubonius* (Di Grande & Scamarda 1973; Bordonaro *et al.* 1984; Di Grande & Neri 1988). This observation, also reported in Malatesta (1985) and Cosentino & Gliozzi (1988), leads to the attribution of a generic Tyrrhenian age to these deposits.

Finally, the Siracusa terrace, above which part of the modern town of Siracusa is built, extends more or less continuously from Fontane Bianche, south of Siracusa, to Augusta (Fig. 4). It is mostly represented by an erosional platform which is well developed along the coastal plains of the Floridia and Augusta basins, where it is carved in the Middle–Upper Pleistocene clays and calcarenites, whereas along the major calcareous headlands (Maddalena, Belvedere, Mt Tauro) it is characterized by a narrow wave-cut platform. In the Belvedere ridge, the Siracusa terrace is bounded landwards by a palaeoshoreline that corresponds to the inner edge of the marine platform, at an elevation of 12 m (Fig. 5a). This line is distinctive across

the whole area, forming a 1–2 m high step in the basin sediments, with notches and small caves along the headland's cliffs. In the Priolo region, however, this line is not distinguishable because of human disruption. To the south, in the Floridia basin, the inner edge of this terrace may be traced at an elevation of 8–10 m, running around the small peninsula of Cozzo Pantano.

2.1.2 Siracusa–Noto area

South of Siracusa, from the southern edge of the Floridia basin to Noto, the individual terrace levels are less distinct. The palaeoshorelines are poorly preserved, extending discontinuously at lower altitudes compared with those occurring in the northernmost area. Close to the northern edge of the Avola fault scarp, palaeoshorelines located at elevations of 105 m and 90 m are easily recognized (Fig. 4). We have correlated these lines, which cap the NW–SE-trending Floridia basin border faults, with the inner edges of the Eurialo and Epipoli terraces, respectively.

From the southern edge of the Floridia basin to the village of Cassibile, a continuous topographic step located at an elevation of 75 m is clearly recognizable (Fig. 4). This feature may correspond to the inner edge of the Tyche terrace, which is represented here by a well developed erosional platform. From Cassibile to Noto this terrace is covered by the debris slope deposits of the Avola fault escarpment. East of Noto

(Fig. 6), patches of terraces characterized by a thin cover of cross-bedded biocalcarenites are correlated with the Epipoli terrace. Small traces of a palaeoshoreline located at an elevation of 25 m correspond to the inner edge of the Neapolis terrace.

On the promontory located east of Cassibile and along the present Avola coastline, an alignment of shoreline notches, mostly carved in the Miocene calcareous substratum at an elevation of 8–10 m, bounds a narrow platform covered by 1–2 m thick biocalcarenites. This thin depositional platform, the sediments of which are the youngest Quaternary marine deposits of the whole area (Di Grande & Raimondo 1982), is correlated with the Siracusa terrace (Fig. 4).

Along the fault escarpment bounding the Floridia basin to the south, two prominent palaeoshorelines are clearly exposed, whereas a large erosional platform lies on the top of the footwall (Fig. 4). The most clearly visible palaeoshoreline is represented by the Spinagallo line, which is characterized by alignments of caves and shoreline notches and extends from SE to NW at elevations ranging from 130 m to about 200 m. This level is marked by the occurrence of a large karst cave, the Spinagallo cave, the floor and the walls of which are covered by thin layers of marine biocalcarenites capped by continental deposits containing mammal fauna (Accordi *et al.* 1959). Along the northern escarpment of the Avola fault, at elevations ranging from 110 to 180 m, there are small traces of further strandlines that could be related to the Grottone 1 and
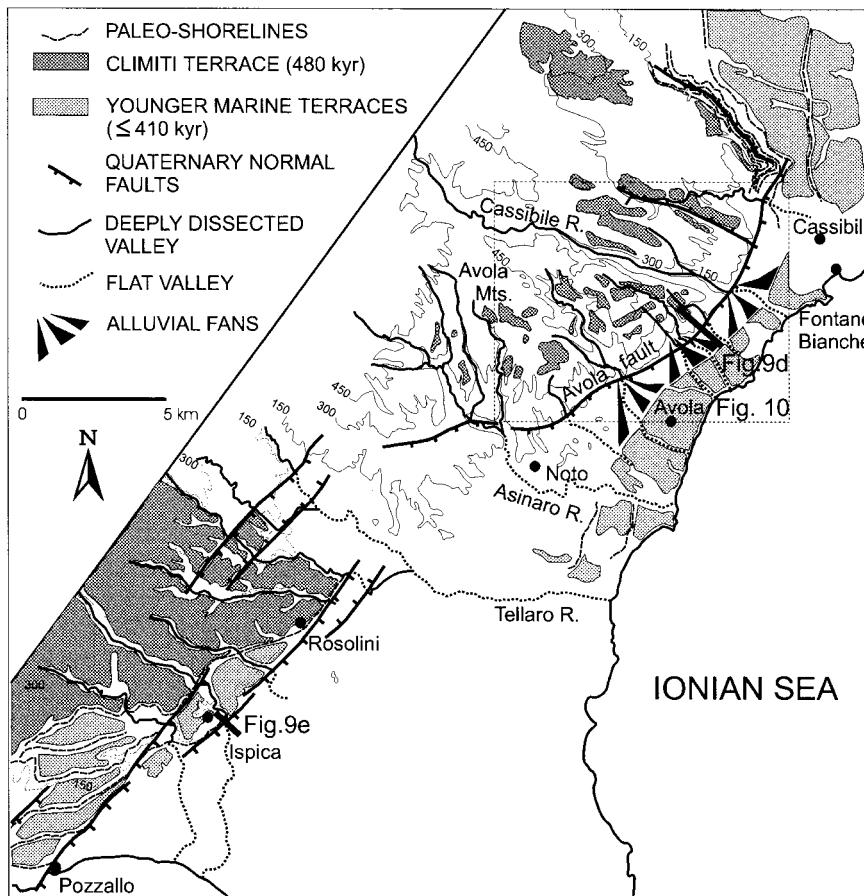

Figure 6. Morphotectonic map of the eastern border of the Hyblean Plateau showing the distribution of marine terraces and palaeoshorelines between Cassibile and Pozzallo (see Fig. 2 for location). The elevation contour lines are from 1:25 000 IGM topographic maps. The locations of the topographic profiles shown in Fig. 9 are also reported.

Grottone 2 levels. On top of the footwall, remnants of a formerly broad erosional platform, now deeply dissected by the drainage network, are clearly exposed (Fig. 6). This surface, here correlated with the Climiti terrace, is warped by antiformal deformation of the footwall of the Avola fault, and varies in elevation from about 170 to 450 m (see below).

Southwards, along the Ispica–Rosolini fault system, only the large wave-cut platform that occurs on the footwall is well preserved, while on the hanging wall the continuity of the terrace levels in the northern part of the area is interrupted (Fig. 6). The lack of terraced surfaces is probably due to the occurrence of soft sediments in the substratum which have subsequently been easily eroded. Nevertheless, morphological observations and the analysis of aerial photographs and SPOT images allow us to correlate the large platform levelling the footwall of the Ispica–Rosolini fault system with the Climiti terrace to the north.

2.2 Age constraints and uplift rates

Absolute age determinations combined with stratigraphic information allow us accurately to define the age of marine terraces exposed along the eastern margin of the Hyblean Plateau (Table 1).

Geochronological data of mammals' teeth collected from continental deposits cropping out along the northern border of the Floridia basin are good constraints for the age of the Akradina terrace. The Akradina biocalcarenites lie above continental deposits containing remnants of *Hippopotamus pentlandi* and *Elephas mnaidrensis*, whose teeth have been dated with ESR (electron spin resonance) geochronological techniques (Rhodes 1996). The ages of the youngest samples collected at this level produce dates with mean values ranging from 74.9 ± 22.2 kyr to 84.5 ± 24.7 kyr, strongly suggesting that the continental deposits were developed during the sea level lowstand corresponding to the OIT stage 5.2. This implies an age of about 80 kyr (OIT stage 5.1), the subsequent marine highstand, for the Akradina terrace (Fig. 3a). The present elevations of the inner edges of the Akradina terrace (32 m), measured in the Belvedere ridge reference area with a -19 m correction (Chappell & Shackleton 1986) with respect to the present sea level, imply an average constant uplift rate of 0.65 mm yr^{-1} in the last 80 kyr for this area. Assuming that this uplift rate was uniform over the Pleistocene period and taking into account, consequently, that a flight of terraces can be considered as linked to the interaction between uplift and sea level change, the ages of the entire flight of terraces can be assessed by correlating the individual palaeoshorelines with the major sea level highstands represented in the eustatic curve. On applying the calculated uplift rate to the eustatic curve we obtain a modified curve in which the expected elevations of the individual palaeoshorelines corresponding to the main sea level highstands are shown (Fig. 5b). Analysis of the eustatic curve adjusted for a 0.65 mm yr^{-1} uplift rate indicates a good correlation between the Siracusa palaeoshoreline and the OIT stage 3.3 (≈ 60 kyr), the Neapolis and Tyche palaeoshorelines with OIT stages 5.3 (≈ 100 kyr) and 5.5 (≈ 125 kyr) and, finally, the Epipoli and Eurialo inner edges with OIT stages 7.1 (≈ 200 kyr) and 7.5 (≈ 240 kyr), respectively. The correlation of the Neapolis terrace with the OIT stage 5.3 is also consistent with the ESR dating of mammals' teeth found in the palaeosoil

levels underlying the biocalcarenites related to the Neapolis terrace (northern border of Floridia basin), which usually gives ages older than 100 kyr (mean values ranging from 120.7 ± 44.5 to 143.6 ± 47.4 kyr; Rhodes 1996).

Despite the occurrence of the Mt Climiti fault, the Grottone 2, Grottone 1 and Spinagallo palaeoshorelines, exposed along the fault scarp, show a good correlation with the marine highstands corresponding to OIT stages 9.1 (≈ 300 kyr), 9.3 (≈ 330 kyr) and 11.3 (≈ 410 kyr) of the proposed modified eustatic curve (Fig. 5b). Isoleucine epimerization ages of teeth of *Elephas falconeri* found in the continental deposits overlying the marine biocalcarenites, deposited on the floor of the karst cave of Spinagallo, give an average age of 455 ± 90 kyr (Belluomini & Bada 1985; Bada *et al.* 1991). The error bar of this absolute age is actually too large to attribute the Spinagallo palaeoshoreline exactly to the OIT stage 11.3, because within this time-window two main marine highstands (OIT stages 11.3 and 13) are included. Moreover, taking into account that (1) the magnitude of the highstand corresponding to the OIT stage 11.3 is considerably greater than the one characterizing the OIT stage 13 highstands, (2) the biocalcarenites of Spinagallo cave are the result of a single marine event, and (3) the time interval between these two stages is particularly short (less than 75 kyr), the attribution of the Spinagallo palaeoshoreline to the OIT stage 11.3 seems to be the more reliable. Wave erosion related to the highstand of the OIT stage 11.3 should have destroyed any sedimentary and morphological record of the previous (lower) highstand (e.g. OIT stage 13). The correlation of the Spinagallo palaeoshoreline with the sea level highstand of 410 kyr (OIT stage 11.3) implies that the continental deposits containing the dated mammal fauna were developed during the subsequent lowstands which may correspond to the OIT stages 11.22 and/or 11.24, the ages of which are included in the youngest portion of the absolute age determination time interval.

The Climiti terrace is the most prominent wave-cut surface directly carved into the calcareous rocks of the eastern border of the Hyblean Plateau, and is the result of protracted erosional processes probably related to distinct sea level highstands. It is thus a suitable candidate for corresponding to the various sea level stands that occurred between ≈ 480 kyr and ≈ 525 kyr during the OIT stage 13 (Fig. 3a). Bearing in mind that in the whole area the palaeoshoreline occurring immediately below this large erosional platform is constantly represented by the ≈ 410 kyr old Spinagallo line, the Climiti terrace, which could have been formed during several cycles related to different marine stillstands, may relate to the latest sea level highstand of the OIT stage 13, corresponding to an age of ≈ 480 kyr.

We consider that the good correlation between the peaks of the modified eustatic curve and the observed elevations of the mapped palaeoshorelines, obtained with an accurate value of uplift rate, are unlikely be accidental, implying that the ages attributed to the entire flight of terraces are reliable.

The chronological determination of the entire flight of terraces, which should, however, be confirmed by future absolute dating, is also supported by the occurrence of three further Holocene palaeocoastlines, two of which occur below the present sea level. The submerged lines have been surveyed a few metres off the present coastlines of the Mt Tauro and La Maddalena peninsulas, at depths of about -2 m and -5–6 m, as also reported by Di Grande & Scamarda (1973). The Holocene coastline occurring onshore extends from Fontane Bianche

to Siracusa: it is represented by a narrow platform which is characterized in places by 1–2 m thick biocalcarenites and is bounded landwards by a well developed inner edge located at about 4 m. According to recent studies of Holocene coastlines carried out along the Tyrrhenian and Ionian coasts (Brancaccio 1968; Antonioli & Frezzotti 1989; Dai Pra & Hearty 1989; Mastronuzzi *et al.* 1989; Alessio *et al.* 1992; Antonioli & Ferranti 1996; Firth *et al.* 1996; Pirazzoli *et al.* 1997; Stewart *et al.* 1997), we can correlate these levels, engraved in the Miocene calcareous rocks, with the very recent minor sea level stands (Fig. 7a) that occurred at 3.5, 6 and about 7 kyr. These stands, according to the Holocene sea level curve proposed by Antonioli & Ferranti (1996) which could be considered representative for southern Italy, were characterized by eustatic levels of -4, 0 and -10 m, respectively. This implies that these strandlines were uplifted with an average rate of 0.6 mm yr^{-1} (Fig. 7b), corresponding to the value obtained from the analysis of the strandlines related to the major Middle–Late Pleistocene sea level highstands. The occurrence of these well-preserved palaeocoastlines related to minor sea level stands could be explained by the very recent age of the lines and by the hard lithology of the host rock.

Uplift rates of about 0.6 mm yr^{-1} in the Holocene are also consistent with the occurrence of the Bronze Age (XIII–XV century) tombs of the Thapsos peninsula (Fig. 4) and the old Greek quarries and harbours (about 700) of Siracusa and La Maddalena peninsula at 1–2 m below the present sea level. Following the regional eustatic curve proposed by Antonioli & Ferranti (1996), which indicates absolute sea levels of -4 m and about -2 m during the Bronze age (3.5 kyr) and the Greek period (2.5–2.7 kyr), respectively, the elevations of these archaeological sites reflect rises of eustatic sea level combined with relatively low rates of tectonic uplift, as also suggested by Firth *et al.* (1996).

The uplift rate has been calculated on the basis of data collected along the reference area of Belvedere ridge. However, this value is not representative for the entire eastern margin of the Hyblean Plateau because the palaeocoastlines of the last six orders of terraces range in elevation from 10 to 50 m over a distance of about 30 km. The uplift rate ranges from mean

values of 0.73 mm yr^{-1} in the Augusta area, north of the Belvedere ridge, to mean values of 0.51 mm yr^{-1} calculated along the southeastern border of the Floridia basin (see Table 1 and Fig. 8).

3 QUATERNARY FAULTING IN EASTERN SICILY

The Quaternary evolution of eastern Sicily has been strongly controlled by normal faulting related to the activity of the southern edge of the Siculo–Calabrian rift zone (Tortorici *et al.* 1995; Mazzuoli *et al.* 1995; Monaco *et al.* 1997). This regional normal fault belt, which runs continuously for 370 km from the northern Calabrian Arc to the Hyblean Plateau, is related to the WNW–ESE-orientated extension that controls the southern regions of Italy. In eastern Sicily the fault belt mostly extends o shore, bordering the uplifted Peloritani mountain range and the Mt Etna–Hyblean region which forms, as a whole, the footwall of this extensional zone (Fig. 1). Moreover, normal faults splay onshore, creating along the eastern slope of Mt Etna the Acireale–Sant'Alfio–Piedimonte fault system (Monaco *et al.* 1997), and along the easternmost part of the Hyblean Plateau the Mt Climiti and lastly the Mt Avola escarpments, and the Rosolini–Ispica fault system (Monaco & Tortorici 1995).

3.1 Onshore structures

The most prominent Quaternary normal faults of southern Sicily occur along the eastern part of the Hyblean Plateau, extending discontinuously along the boundary between the plateau and the adjacent coastal plains. This 70 km long fault belt, here named the Eastern Hyblean Fault Belt (EHFB), is made up of several NW-trending (Mt Climiti fault system and Floridia basin border faults) and NE-trending (Avola fault and Rosolini–Ispica fault system) fault segments that control the present topography, showing steep escarpments with very sharp morphology.
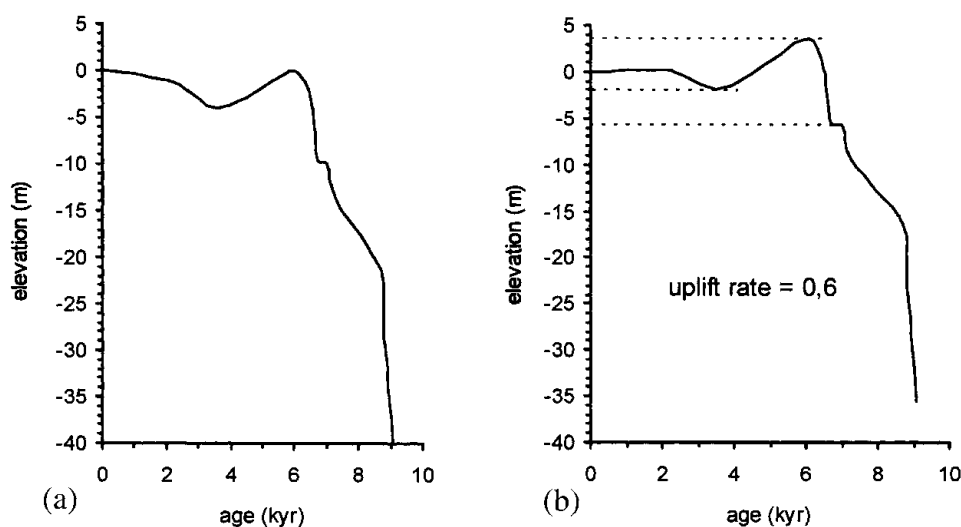

Figure 7. (a) Holocene eustatic curve defined for the Tyrrhenian Sea (from Antonioli & Ferranti 1996), and (b) corrected for an uplift rate of 0.6 mm yr^{-1}. Dashed lines in (b) show the expected elevations of shorelines correlated to marine stands occurring at 3.5, 6 and about 7 kyr.
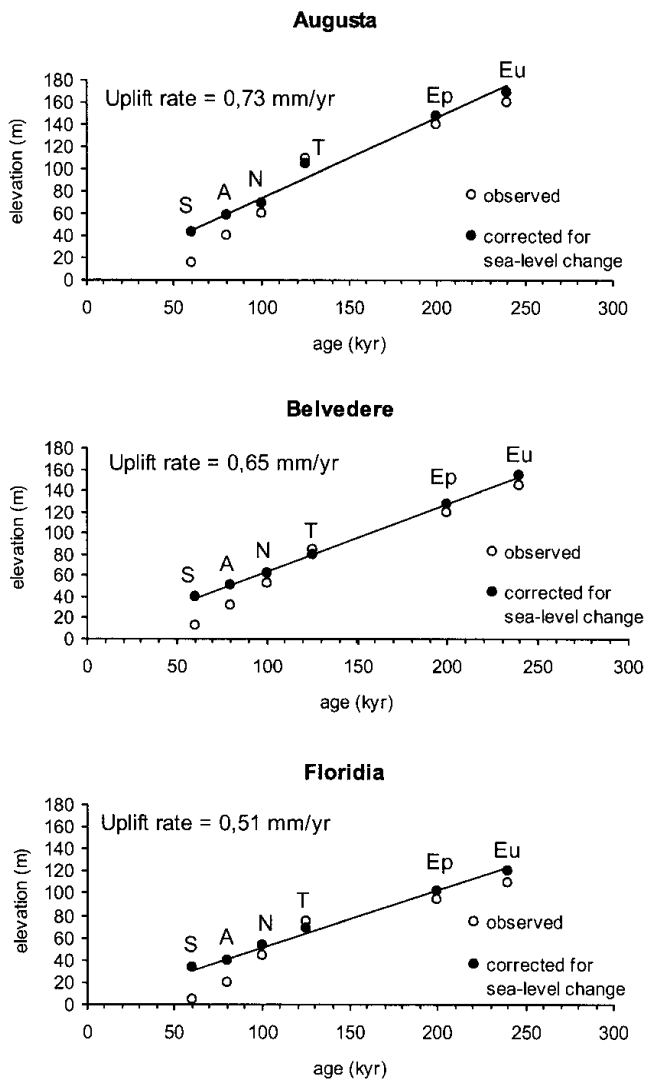
Figure 8. Diagrams showing uplift rates characterizing the areas of Augusta, Belvedere ridge and the southern part of the Floridia basin. Uplift rates are obtained for the last 240 kyr by fitting the elevations of the inner edges of the Siracusa (S), Akradina (A), Neapolis (N), Tyche (T), Epipoli (Ep) and Eurialo (Eu) terraces corrected for sea level changes.

3.1.1 Mt Climiti fault system

The northern branch of the EHFB is made up of several NW-trending fault segments that extend for about 35 km from Augusta to south of Siracusa, defining a series of tectonic depressions filled by Quaternary sediments (Fig. 4). The major normal fault segment strikes N150°E and runs for about 15 km along the base of Mt Climiti (Mt Climiti fault) from Melilli to a few kilometres west of Siracusa. It exhibits a 150–170 m high linear escarpment characterized by a down convex-shaped profile (Fig. 9a). To the west, the Mt Climiti fault is accompanied by a few SW-dipping normal fault segments which, stepping into the uplifted block, produce a footwall ridge which separates the Pleistocene basin that extends along the coastal plain (Augusta–Siracusa basin) from the Floridia depression (Fig. 4).

The uplifted footwall ridge is characterized by Oligocene–Miocene calcareous sediments above which remnants of the

480 kyr old Climiti wave-cut platform extend at an elevation of 400 m. The Mt Climiti fault plane dips eastwards at about 70° and is characterized by a 40 m wide cataclastic belt along which a decimetre-spaced fracture cleavage is well developed. Lower–Middle Pleistocene calcarenites and clays occur in the down-dropped blocks where six different main Late Quaternary strandlines are developed. These are accompanied by their respective marine terraces and wave-cut platforms (Di Grande & Raimondo 1982; Bordonaro *et al.* 1984) ranging in elevation from about 15 to 160 m. The shoreline corresponding to the inner edge of the Eurialo terrace extends at elevations of 160 m. It is carved in the well-cemented alluvial wedge that developed continuously at the base of the Mt Climiti fault scarp, sealing the west-dipping antithetic structures (Fig. 4). The fault escarpments that border the Mt Climiti ridge are engraved by the alignments of marine caves belonging to the Spinagallo, Grottone 1 and Grottone 2 palaeoshorelines. Taking into account, moreover, that uplift rates on the Mt Climiti footwall have equalled those on the hanging wall (see above), the fault activity of the Mt Climiti fault is inferred to be older than ≈410 kyr.

Eastwards, between Augusta and Siracusa, distinct westward-dipping antithetic normal fault segments isolate an ≈16 km long, ≈10 km wide tectonic depression (Augusta–Siracusa basin). Fault segments mostly extend offshore, very close to the coastline to be exposed onland along the western slope of the Mt Tauro and Thapsos peninsulas (Fig. 4). The backbone of the uplifted blocks, which are tilted eastwards by about 5°, is made up of Miocene carbonate sediments unconformably covered by Middle Pleistocene calcarenites (Bordonaro *et al.* 1984). The Augusta–Siracusa basin is indeed filled by a Lower–Middle Pleistocene sequence made up of a basal level of calcarenites capped by 70 m of clays and marly clays sediments. This sequence is unconformably covered by Upper Pleistocene calcarenites (Bordonaro *et al.* 1984) that represent the deposit related to the 100 kyr old Neapolis terrace and onlap the escarpment of the Mt Tauro fault segment in the east. This implies that the Quaternary activity of fault segments that bound the Augusta–Siracusa basin in the east was older than the Late Pleistocene. The Mt Tauro fault segment exhibits a sinuous and degraded scarp (Fig. 9b) which is notched by the inner edge of the Akradina terrace that extends at a uniform elevation of 30 m across both the hanging wall and footwall (Fig. 4).

3.1.2 Floridia Basin border faults

A few kilometres south of Siracusa, a west-dipping normal fault running along the slope of the Maddalena peninsula bounds the Floridia basin to the east (Fig. 4). This basin is filled by Lower–Middle Pleistocene calcarenites and clays unconformably capped by Upper Pleistocene calcarenites (Di Grande & Raimondo 1982) which onlap the fault plane eastwards thus postdating its activity. The fault scarp exhibits a smoothed profile (Fig. 9c) and bounds the uplifted block of the La Maddalena peninsula which is mostly made up of Miocene carbonates above which remnants of the Neapolis and Akradina terraces extend at elevations of 45 and 20 m, respectively.

To the southwest, the Floridia basin is also bounded by a NE-dipping, NW–SE-trending normal fault which shows a very
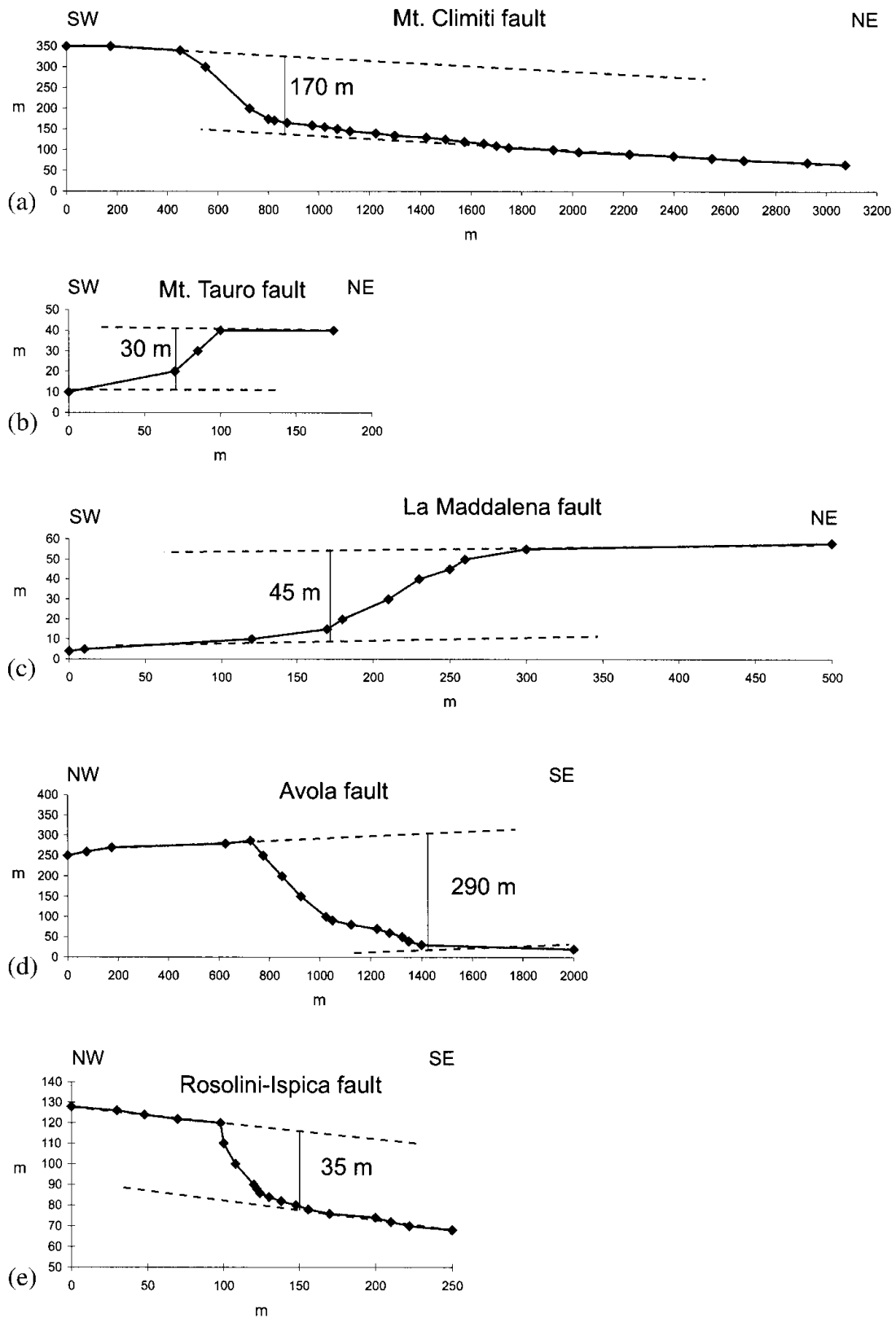
Figure 9. Topographic profiles traced from Regione Siciliana 1 : 10 000 maps across normal fault segments along the eastern border of the Hyblean Plateau (for location see Figs 4 and 6).

smooth escarpment, suggesting that during Late Quaternary times the erosional processes were predominant over the tectonic movements. This border fault, which is cut by the Spinagallo, Grottone 1 and Grottone 2 palaeoshorelines marked by alignments of large marine caves, is accompanied by a further NE-dipping normal fault segment which steps into the uplifted block and o sets the large Climiti wave-cut platform developed on the footwall (Fig. 6). As with the Mt Climiti fault system, the activity of Floridia border faults can be considered older than about 410 kyr. The time of faulting at Mt Tauro, Thapsos and La Maddalena is older than the sediments related to the 100 kyr old Neapolis terrace. Actually, these fault segments could have been active until about 410 kyr, by their having emerged only since 100 kyr and thus not recording the older events connected with the eustatic sea level changes.

3.1.3 Avola fault

Along the southern edge of the Hyblean Plateau, the EHFB swings in a NE direction between Cassibile and Pozzallo (Fig. 6). The major segment of this branch is represented by a 20 km long, east-dipping normal fault (Avola fault) that clearly cuts the NW–SE-trending Floridia basin border faults, extending from Cassibile to Noto, and separates the Avola mountains from the coastal plain (Fig. 6). The uplifted footwall is made up of Miocene carbonates directly overlain by remnants of the large Climiti erosional platform. On the hanging wall, the Miocene deposits are unconformably covered by the Upper Pleistocene beach calcarenites that form the two distinct orders of the Tyche and Neapolis marine terraces, the inner edges of which are located at 50 and 25 m, respectively.

The Avola fault (Fig. 10) controls the present topography, showing a steep escarpment with very sharp, mostly Late Pleistocene to Holocene, morphology. It is defined by a linear cumulative scarp characterized along the strike by di erent heights which, on reaching the maximum value of 290 m near the centre of the fault segment (Fig. 9d), progressively decrease towards its northern and southern edges (see profile in Fig. 10). O set variation occurring along the fault strike is well recorded in the footwall, which is clearly a ected by a large antiform, with a generally perpendicular axial trace with respect to the fault plane, and a hinge zone located around the centre of the fault where the o set reaches its maximum values. Antiformal deformation is emphasized by the variation in elevation of the large erosional platform of the Climiti terrace cut on top of the footwall (Fig. 10). This platform, the age of which predates the activity of the Avola fault, extends from about 170 m close to the fault tips to 450 m on the hinge zone. On the hanging wall, along the escarpment which exhibits triangular facets, large, still active, alluvial fans are well developed. The drainage network flows almost perpendicular to the fault trace and it is made up of deeply entrenched and large flat valleys in the uplifted footwall and down-dropped hanging wall (Fig. 6). On the footwall, the drainage network is formed by two distinct stream generations (Fig. 10) whose evolution may be related to the activity of the Avola fault. The first and oldest stream generation is represented by several kilometre-long rivers (e.g. the Cassibile River) that cross the entire Hyblean Plateau with deep-sunken meanders flowing within spectacular canyons which, close to the fault trace, reach heights of about 250 m. These streams, which erode the terrace platform extending over

the footwall, therefore represent antecedent rivers that predate the severe uplift of the footwall. The second stream generation comprises about 1 km long, rectilinear, deeply entrenched channels which represent the evolution of funnel-shaped gullies and develop as a direct response to the fault-generated scarp.

The activity of the Avola fault is thus predated by the oldest stream drainage generation which, by incising the footwall wave-cut platform related to the 480 kyr old Climiti terrace, probably developed during the subsequent marine lowstand that occurred about 430 kyr ago, corresponding to the OIT stage 12 (Fig. 3a). The Avola fault, moreover, clearly cuts the southern border faults of the Floridia basin, thus implying that most of its activity was younger than 410 kyr and continued until the Holocene, as suggested by the morphological features of the fault escarpment.

3.1.4 Rosolini–Ispica fault system

Finally, to the south, the EHFB is made up of a N30°E-trending array with steep, mostly east-dipping, master planes (Rosolini–Ispica fault system) that to the east bound the southern edges of the Hyblean Plateau (Fig. 6). Near the town of Rosolini, an antithetic fault segment isolates a 4 km long, 1 km wide graben. The Rosolini–Ispica fault system comprises two main left-stepping fault segments characterized by very sharp, linear scarps which extend for a total length of about 20 km and reach heights of 35 m (Fig. 9e). The fault escarpments o set the large wave-cut platform surface of the Climiti terrace. This cuts the Oligo-Miocene carbonates and extends over a total length of 8 km, at an elevation ranging from about 150 m close to the fault plane to about 320 m along its inner edge. Antecedent streams forming deeply entrenched channels and scarp-related gullies characterize the uplifted blocks, whereas a di use and unentrenched drainage network developed on the hanging wall block. These morphological features indicate a very young, mostly Late Pleistocene to Holocene activity for the Rosolini–Ispica fault segments. This age is also confirmed by the occurrence on calcareous bedrock of a 0.5 m high, light-coloured scarplet, which extends for about 4 km along the base of the fault escarpment near Rosolini and was probably related to the occurrence of a seismic event, as is the case along other active normal faults in Afar (Tapponnier *et al.* 1990), in Greece (Armijo *et al.* 1991, 1992; Stewart & Hancock 1991), and in Italy (Piccardi *et al.* 1999).

3.2 Offshore structures

The geometry of the fault segments extending o shore in the Ionian Sea has been defined by the analysis and the interpretation of 13 seismic reflection profiles. These include eight deep penetration seismic lines (lines A, B, C, 1, 2, 3, 4 and 5) recorded between 1993 and 1995 during the project ETNASEIS and published in Hirn *et al.* (1997), four single channel profiles (J1, J22, J42 and Me2) published in Scandone *et al.* (1981) and Sartori *et al.* (1991), and an older multichannel line (MS 27).

The reflection lines (Fig. 11) depict a grid formed by four NNE–SSW-trending profiles (lines A, B, C and Me2) extending parallel to the coast from Catania towards the Straits of Messina, six E–W-orientated lines (1, 2, 4, 5, J1 and J22)
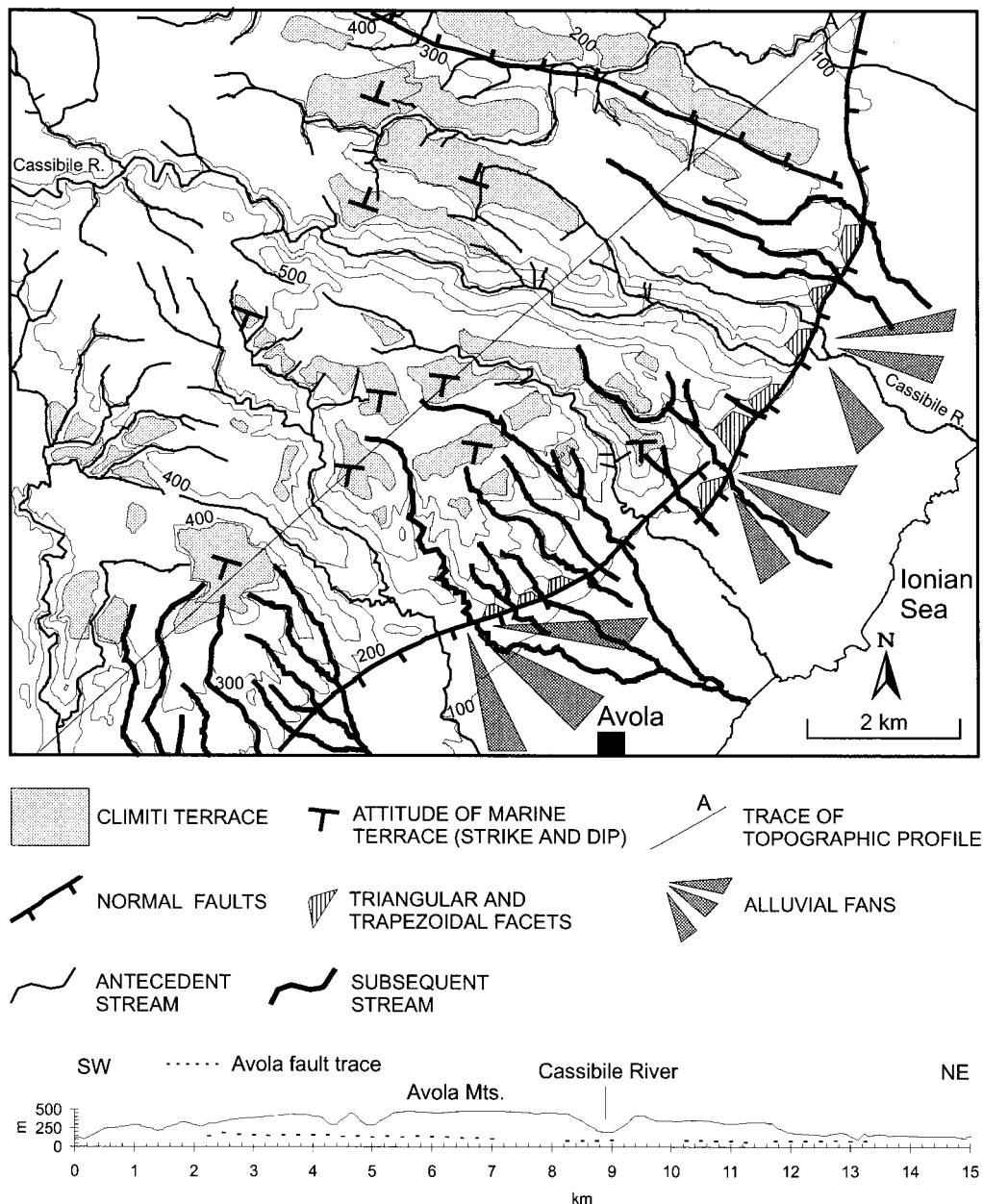
Figure 10. Morphotectonic map of the Avola mounts (for location see Fig. 6). A topographic profile of the crest line of the footwall and the projection of the Avola fault topographic profile is shown below.

which, running perpendicular to the coastline, explore the Ionian Sea portion from Catania to Siracusa, two NW–SE-trending profiles (3 and MS27) which extend from the southeastern slope of Mt Etna towards the Ionian plain, and, finally, one N–S line (J42) which runs parallel to the coast from Augusta to Noto.

The most impressive feature shown by the seismic lines is the occurrence, at a shallow depth, of a number of eye-shaped half-grabens which, bounded westwards by east-facing normal fault segments, constitute sedimentary basins infilled by synrift clastic wedges that thicken towards the boundary fault (Fig. 12). At depth, the faults, which dip eastwards by 60°–70°, terminate in the highly reflective zone that is located in the hanging wall at 6–9 s two-way traveltime (twt) and which is

considered to represent the laminated lower crust/mantle boundary of the Ionian domain (Cernobori *et al.* 1996; Hirn *et al.* 1997). Normal faults mostly develop within the thinned crust of the Ionian domain, partially re-activating the Malta Escarpment, south of Augusta.

The detailed analysis of the profiles together with the basin distribution allows definition of the structural pattern that characterizes the Ionian o shore zone close to eastern Sicily (Fig. 13). In the southern part of the investigated area, the o shore zone from Siracusa to Catania, the fault segments strike along a NNW direction showing an overall right-hand en échelon arrangement, whereas in the northern part they swing along a NNE direction linking with the Straits of Messina fault zone (see Fig. 1).
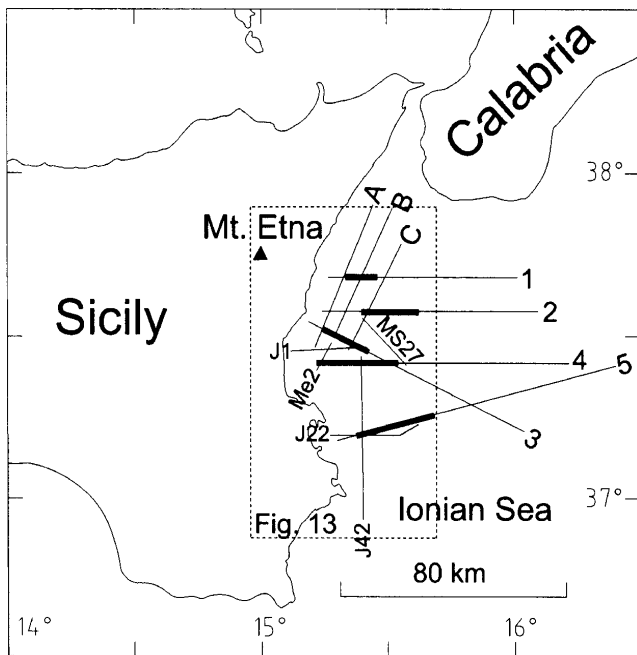
Figure 11. Locations of seismic profiles carried out in the Ionian offshore area of eastern Sicily. Thicker lines refer to seismic profiles reported in Figs 12, 14, 15 and 17.

The distinct fault segments are arranged to form two large eastward-convex arc-shaped major fault segments which bound the different sedimentary basins. Along the eastern fault, corresponding to the F6 fault described by Hirn *et al.* (1997) and which extends for a length of about 50 km, the sedimentary basins occurring on its hanging wall, as shown by the lines 2 and MS27, are well developed.

In line 2, which clearly shows the fault trace, three main seismostratigraphic units, representing the prerift and synrift sequences, can be easily distinguished (Fig. 12). The top of the Meso-Caenozoic carbonate succession is represented by a west-dipping (about 20°) reflection (horizon M) recognizable at 4.4–3.7 s twt. Above it, a band of well-defined reflections, confined between the horizons P at the bottom and Q at the top, is clearly recognizable between 4.2 and 3.5 s twt. The horizons M and P bound a seismostratigraphic interval which is characterized by low reflectivity and has been interpreted in the Ionian domain (Sartori *et al.* 1991) as constituting the Lower Pliocene sediments (Trubi Formation). These two seismostratigraphic intervals, confined between the horizons M and P, and P and Q, show a uniform thickness and represent the pre-rift sequence. These intervals along the fault surface are severely deformed, forming a well-developed drag hanging wall syncline (Fig. 12). The upper portion of the section, above the horizon Q, shows a wedge-shaped interval characterized by a set of eastward onlapping reflections that is interpreted as the infilling of a synrift basin related to the fault activity. Furthermore, line 2 shows that the fault trace offsets the seafloor, thus implying that fault activity that occurred mostly during the deposition of the seismostratigraphic interval bounded by the Q horizon and the seafloors may have continued up to the present. Isochronopachs of this seismostratigraphic interval, as derived from the analysis of the seismic lines, show that the synrift basins related to the eastern fault activity are characterized by lengths of up to 15 km extending to depths of about 0.9 s twt.

The western master fault, which corresponds to the F4 fault of Hirn *et al.* (1997), runs 12 km offshore, extending parallel to the coastline, from Siracusa to Catania, for a total length of about 50 km (Fig. 13). The synrift basins, which are smaller in size (both in length and depth) than that developed along the eastern fault, mostly occur along the northern branch of the main fault segment, reaching lengths of 10 km and extending to depths of 0.6 s twt. The seismic lines 3, 4, 5, J1 and J22 (for the J lines see Fig. 3 in Scandone *et al.* 1981) clearly show the fault trace with the sedimentary basins on the hanging wall. Horizons M, P and Q are easily recognizable in all the sections defining the prerift and the synrift seismostratigraphic intervals described in line 2. Roll-over anticlines deform, in places, the prerift sequence, as shown in line 4 (Fig. 14).

All the seismic lines show that the western fault offsets the seafloor (Figs 14 and 15), cutting the thinned crust of the Ionian domain along the northern branch and re-activating the Malta Escarpment to the south (lines 4 and 5).

Depth conversions of the M, P and Q horizons and thickness evaluations of the intervals bounded by the above-mentioned horizons were based on interval velocities computed during seismic data processing. Using an interval velocity diagram that can be considered as representative for the entire prospected area (Monaco *et al.* 1995), velocities of 1750, 2800 and 3000 m s^{-1} were used for the intervals bounded by the horizon Q and the seafloor, by the horizons P and Q, and finally by the horizons P and M (Fig. 12). These data suggest a thickness of 200–250 m for the Trubi Formation and of about 800 m for the deposits included between the horizons P and Q, whereas a maximum thickness of 700 and 800 m could be assumed for the synrift sedimentary wedges infilling the basins that occur along the eastern and western master faults, respectively.

The information derived from the analysis of the seismic lines, combined with surface geological data and available logs related to deep wells drilled for oil exploration in the Catania plain, allows the various seismostratigraphic intervals to be defined. According to its seismic properties, the interval bounded by the horizons M and P is interpreted as belonging to the Trubi Formation. This implies that the seismostratigraphic interval sandwiched between horizons P and Q represents Pliocene–Pleistocene sediments which, according to its velocity of 2800 m s^{-1}, could be formed by a sequence of prevalent claystones. A monotonous sequence of clays and marly clays, containing in its lower levels calcarenites and several lens-shaped bodies of volcanics, crops out onland along the coast from the eastern slope of Mt Etna to the Hyblean Plateau, and is also found at depth for about 900 m in the Catania 1, 5, 9 and 10 wells (Longaretti *et al.* 1991). The base of this sequence, which rests unconformably above both the Meso-Caenozoic carbonates and the Lower Pliocene Trubi Formation, is of Middle Pliocene age, whereas in the upper portion radiometric determinations carried out in the interlayered volcanic rocks indicate (Gillot *et al.* 1994) a Middle Pleistocene age (about 520 ± 20 kyr). Moreover, the uppermost part of this clayey sequence is characterized by the occurrence of lens-shaped bodies of sand and conglomerates containing clasts of volcanic rocks (Kieffer 1971; Monaco 1997) having an age, obtained by K–Ar determinations (Gillot *et al.* 1994), of 300 ± 65 kyr. Taking into account that this sequence is capped by terraced deposits attributed by Kieffer (1971) to the Mindel–Riss interglacial (OIT stage 9.3; 330 kyr), these data
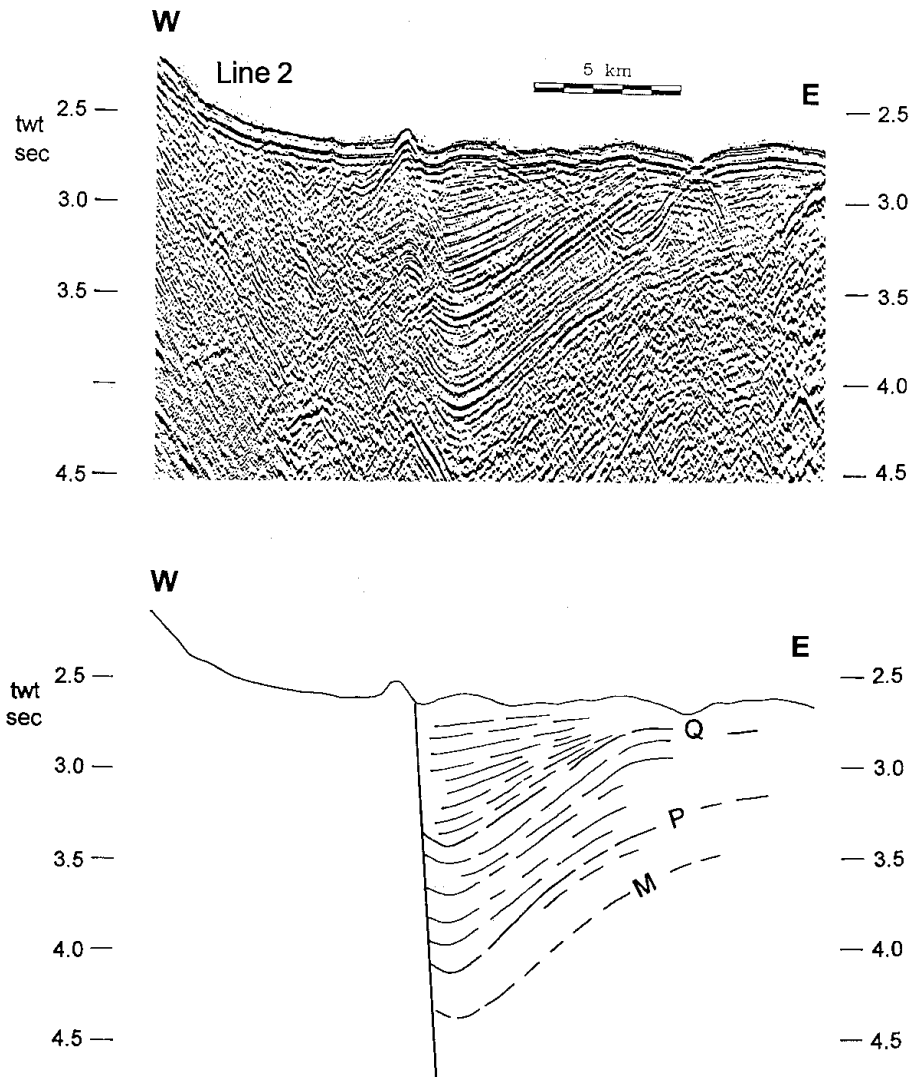
Figure 12. Reflection seismic profile 2 (for location see Fig. 11) and line drawing showing the thick sedimentary basin developed on the hanging wall of the major normal fault segment. Horizon M marks the top of the Meso–Cenozoic carbonates, whereas horizon P bounds the top of a seismostratigraphic interval characterized by low reflectivity, which has been interpreted as constituting the Lower Pliocene sediments (Trubi Formation). Horizon Q marks the base of a wedge shaped interval characterized by a set of eastwards onlapping reflections which is interpreted as the infilling of a synrift basin related to the fault activity. The two seismostratigraphic intervals confined between the horizons M and P and P and Q show a uniform thickness and represent the prerift sequence, which is severely deformed along the fault surface, forming a well developed drag hanging wall syncline.

strongly suggest an age ranging between the Middle Pliocene and the Middle Pleistocene (about 330 kyr   ) for the P–Q seismostratigraphic interval.

The synrift sedimentary wedges exhibit a velocity of $1750 \, \text{m s}^{-1}$ and could correspond to loose clastic deposits. They are therefore attributed to an age ranging between the Middle Pleistocene (about 330 kyr   ) and the Holocene. This time span includes several sea level lowstands characterized by a very high erosional rate, which strongly supports the idea that the thick sedimentary wedges infilled the basins located along the hanging walls of the major faults (Fig. 13).

Seafloor displacements occurring along the major faults are clearly visible on the lines 3, 4 and 5 which show, along the southern edge of the western fault, well developed steep scarps that reach heights ranging from about 80 to 240 m. They suggest a fault reactivation of the older Malta Escarpment (Figs 14 and 15).

3.3 Slip rates on Quaternary faults

The morphological and geological features of the most recent fault segments occurring both onshore and o shore in the eastern margin of the Hyblean Plateau, together with the age determination of the marine terraces, provide very good information for evaluating slip rates. The unconstrained timing of activity on the older fault system (Mt Climiti fault system and Floridia border faults) makes definition of slip rates along these segments impossible.

Onshore, the Avola fault has been active at least since 410 ka, and shows a 290 m high cumulative scarp (Fig. 9d), thus implying a maximum long-term vertical uplift rate of $0.7 \, \text{mm yr}^{-1}$. As for the Rosolini–Ispica fault, we are not presently able to indicate any values of slip rate because of the lack of available chronological data.
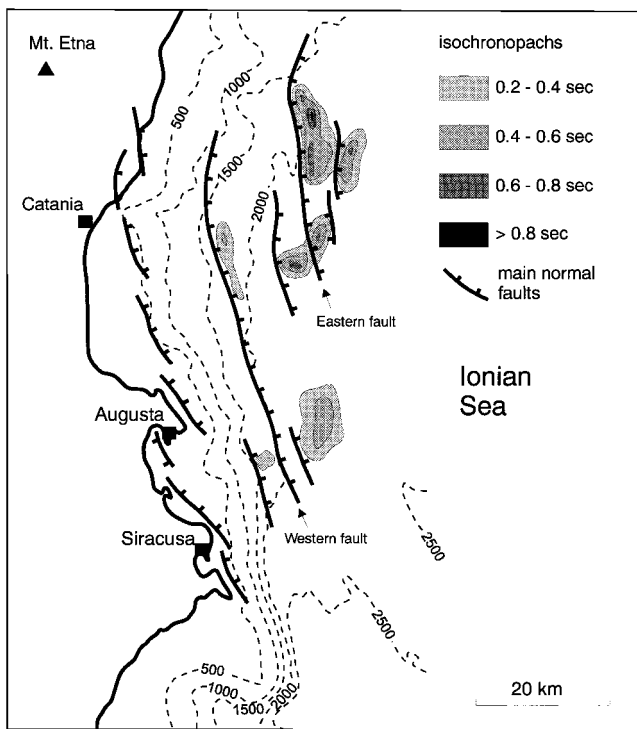
Figure 13. Structural sketch map of the Ionian o shore zone of eastern Sicily (for location see Fig. 11) derived from the analysis of seismic reflection profiles. Isochronopachs of the seismostratigraphic interval included between the horizon Q and the seafloor show the overall geometry of the main eye-shaped synrift basins developed along the hanging wall of the major normal fault segments.

Slip rates on the fault segments extending along the Ionian o shore have been evaluated by using both a direct analysis of the seismic profiles and the distribution of deformation of the uplifted footwall, which can be explained by assuming a flexural cantilever model of fault deformation. This model describes the fault-controlled deformation a ecting an elastic layer (e.g. the upper crust) lying above a viscous half-space (e.g. the middle and lower crust) (King *et al.* 1988; Stein *et al.* 1988; Kusznir *et al.* 1991; Roberts & Yielding 1991; Armijo *et al.* 1996). In this model, the cumulative deformation associated with the activity of the major fault approximates to the summation of repeated cycles of movements which correspond to coseismic and postseismic earthquake deformation related to cycles of earthquakes. Long-term flexural deformation, which depends on the e ective elastic thickness of the faulted layer, a ects both the hanging wall and the footwall and is distributed across a zone tens of kilometres wide (Fig. 16). Considering that in southeastern Sicily the thickness of the elastic layer (the upper crust), which ranges between 13 and 18 km (Makris *et al.* 1986; Hirn *et al.* 1997), is similar to that used by King *et al.* (1988) in theoretical modelling and by Armijo *et al.* (1996) to describe the crust deformation of the Corinth area, our data (length and dip of fault plane, footwall uplift and hanging wall downdrop) have allowed us to construct a long-term deformation curve in agreement with the flexural cantilever model.

According to the model, the total vertical displacement along the fault plane is represented by the total amount of footwall uplift and hanging wall collapse. Besides clearly

depicting fault and basin geometry and the thickness of the synrift sequences, seismic profiling in the Ionian seaboard also shows well preserved fault scarps bounding the uplifted footwall. These fault scarps, entirely developed under a water column of about 1500–2000 m, were preserved from significant erosional processes. Seismic line 1 (Fig. 17) is likely to evaluate the footwall uplift/hanging wall downdrop ratio (u/d) with an accuracy of ± 20 m related to the vertical resolution of the seismic signal. In this line, a well preserved fault scarp 330 ± 20 m high and a sedimentary synrift wedge that reaches a total thickness of 530 ± 20 m are shown. Taking into account that the uncertainty in thickness measurements corresponds to an error bar ranging within the bounds of ± 5 per cent, and assuming that the basin floor has been maintained at its original level by sedimentation (as opposed to the underfilled or overfilled basin), the values measured on the seismic line imply an average u/d ratio of 1/1.6, which is tentatively applied to the entire set of o shore fault segments.

On the western fault, the hanging wall synrift sediments deposited during the last 330 kyr show a total thickness of about 630 m (see isochropachs of Fig. 13 and lines 3, 4 and 5 shown in Figs 14 and 15). This value, which represents the vertical displacement of the down-dropped block, combined with the u/d ratio of 1/1.6 gives a footwall uplift of 390 m, thus implying a total amount of vertical displacement of 1020 which suggests a long-term total vertical slip rate of 3.1 mm yr^{-1} on the western fault during the last 330 kyr. The long-term vertical slip rate related to the uplift of the footwall during this time span consequently assumes a value of 1.2 mm yr^{-1}, which represents the tectonic vertical rate estimated on the fault plane.

This value, together with the uplift rates obtained from the analysis of the marine terraces occurring along the eastern margin of the Hyblean Plateau (see Table 1 and Fig. 8), allows us to define the long-term deformation of the entire footwall of the western fault. The values of the uplift rates calculated on the fault plane and at 25 km (Augusta area), 30 km (Belvedere ridge) and 40 km (southeastern border of the Floridia basin) from the centre of the western fault fit along a curve that reaches the value of 0 at a distance of 90–100 km from the fault plane (Fig. 18). This curve does not, however, correspond to the theoretical models of long-term deformation (King *et al.* 1988), which, for a 45 km long fault, predict a fault-related deformation up to a maximum distance of about 60 km from the fault plane. According to the theoretical model, we assume that the uplift rate of 0.26 mm yr^{-1} defined by the curve at 60 km from the fault plane may correspond to a regional uplift component of the area. On this basis, the values of uplift rates corrected for the regional uplift define the curve of the long-term deformation related to the Quaternary activity of the western fault (Fig. 18), being consistent with both the long-term theoretical curves (King *et al.* 1988) and the observed terrace profiles carried out for the Corinth rift zone (Armijo *et al.* 1996).

The value of the long-term vertical uplift rate of 3.1 mm yr^{-1} (U in Fig. 19) on the western fault corresponds to a dip-slip rate on the fault plane, which dips westwards at about 60°–70°, of 3.4 ± 0.2 mm yr^{-1} (Ds in Fig. 19).

Taking into account that the western fault strikes N160°E, thus forming an angle of about 60° with respect to the N100°E regional extension direction measured on the eastern slope of Mt Etna (Monaco *et al.* 1995), a 25–35 per cent right-lateral
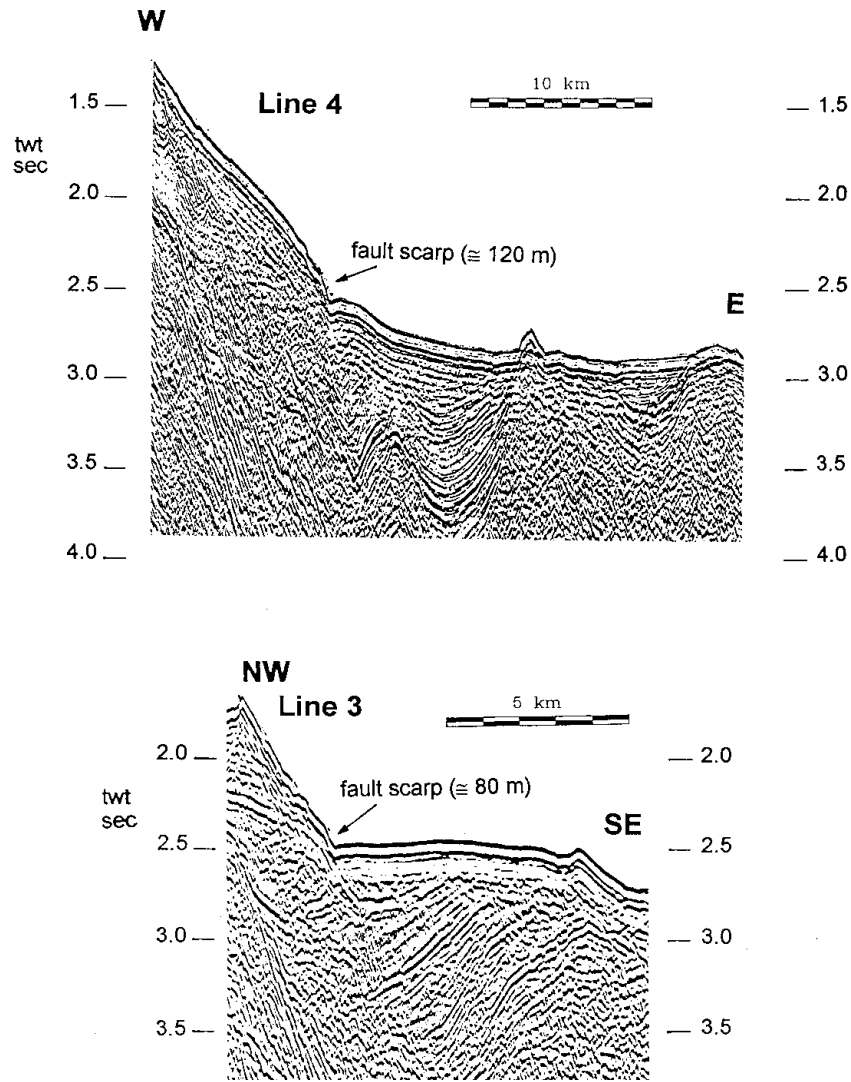
Figure 14. Reflection seismic profiles 3 and 4 (for location see Fig. 11) showing the synrift basins developed along the hanging wall of the western fault. The thick line indicates the horizon Q. In line 4, a well developed roll-over anticline a ecting the prerift sequence is shown. Profiles also show the western fault, which o sets the seafloor and re-activates the pre-existing Malta Escarpment (line 4) forming well-exposed scarps.
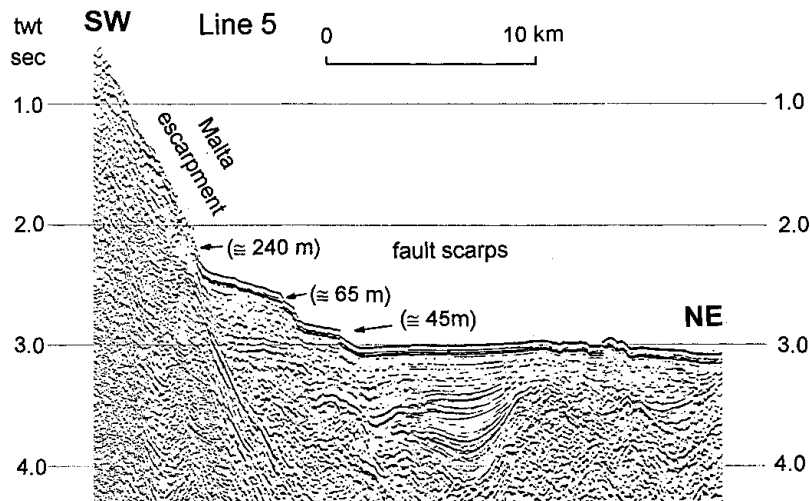

Figure 15. Reflection seismic profile 5 (for location see Fig. 11) showing the western master fault which, accompanied by minor synthetic fault segments, bounds a well developed synrift basin eastwards, and re-activates the older Malta escarpment, displacing the seafloor with a cumulative well defined scarp of about 350 m.
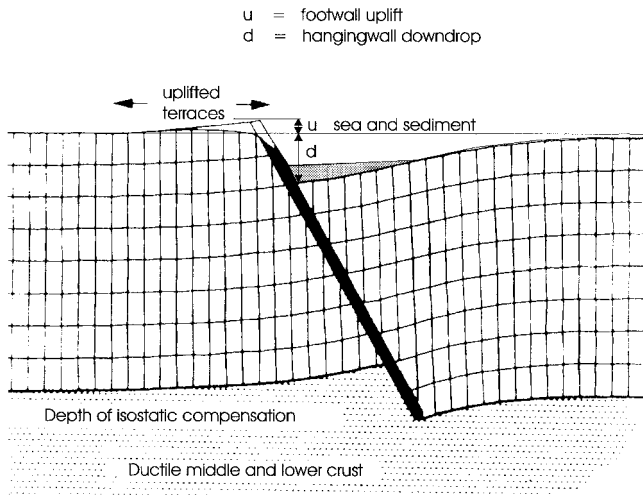
Figure 16. Geometry of downthrown and uplifted blocks predicted by the flexural cantilever deformation model (modified from Armijo *et al.* 1996).
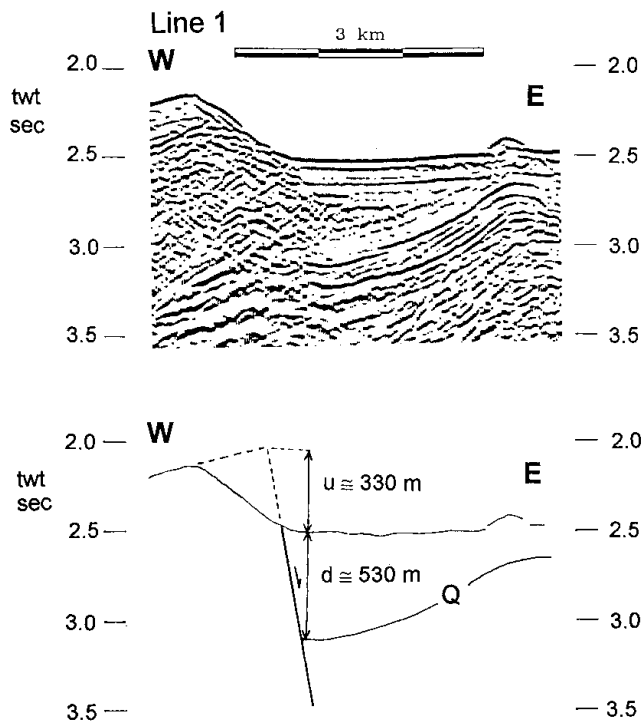

Figure 17. Reflection seismic profile 1 (for location see Fig. 11) and schematic line drawing depicting fault and basin geometry. The line, which shows a well preserved fault scarp separating the uplifted footwall from the synrift basin, bounded at the base by horizon Q, provides quantitative data to evaluate the footwall uplift/hanging wall downdrop ratio (u/d).

component of motion along the fault plane is to be expected. This implies that the net slip rate along the plane of the western fault assumes values of 3.7 ± 0.3 mm yr^{-1} (S in Fig. 19). These values are consistent with the large-scale motion recorded in the Hyblean Plateau by the VLBI network, which shows horizontal velocities of about 7 mm yr^{-1} for the site of Noto (Ward 1994). Similar vertical slip rates have been recorded along the normal fault segments occurring in the Corinth rift
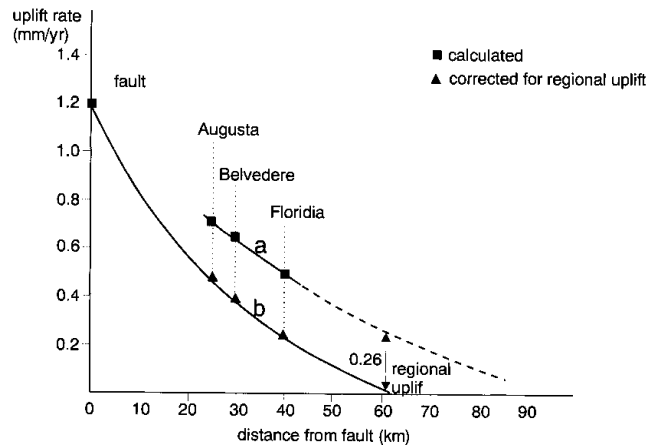
Figure 18. Best-fitting curves for cumulative (curve a) and fault-related (curve b) uplift rate values of the footwall of the western fault.

zone (Armijo *et al.* 1996), whereas they are considerably higher than those observed along the normal faults occurring in the central Apennines and Calabrian Arc (Tortorici *et al.* 1995; Michetti *et al.* 1996; Piccardi *et al.* 1999).

4 THE 1693 EARTHQUAKES

Between 1693 January 9 and 11, the whole of southeastern Sicily was devastated by two large earthquakes of MCS intensities VIII–IX and XI, respectively. The main shock, which is reported (Baratta 1901; Postpischl 1985a; Boschi *et al.* 1995a) as the largest seismic event ever recorded in the central Mediterranean, occurred on January 11 and was felt in southern Italy (Lucania, Puglia, Calabria) and as far south as Malta, and along the coastal region of Tunisia. This sequence has usually been reported as a single earthquake characterized by a mesoseismal area including the cumulative effects of the two shocks (Baratta 1901; Postpischl 1985b). Indeed, a detailed analysis of the effects of the two distinct shocks (Boschi *et al.* 1995a) provides useful information to better define the possible active faults associated with the seismic events.

4.1 January 9 event

The first shock, which occurred at about 9 pm (GMT), caused severe damage to the small towns of Noto Antica, Avola Antica, Floridia, Melilli, Lentini and Carlentini. These towns, whose MCS intensities have been evaluated as VIII–IX (Boschi *et al.* 1995a), form a narrow belt (Fig. 20a) extending along the eastern border of the Hyblean Plateau (Avola and Climiti Mounts). This belt is surrounded by a large area, including the towns of Catania, Brucoli and Francofonte, where the earthquake caused minor damage. This area, which was characterized by an MCS intensity of VIII (Boschi *et al.* 1995a), includes the town of Augusta, which was severely struck with an MCS intensity of VIII–IX (Boschi *et al.* 1995a). This anomaly is probably caused by a local seismic response related to the geological features (site conditions) characterizing the town of Augusta, which was built on unconsolidated sediments (loose calcarenites and clays).
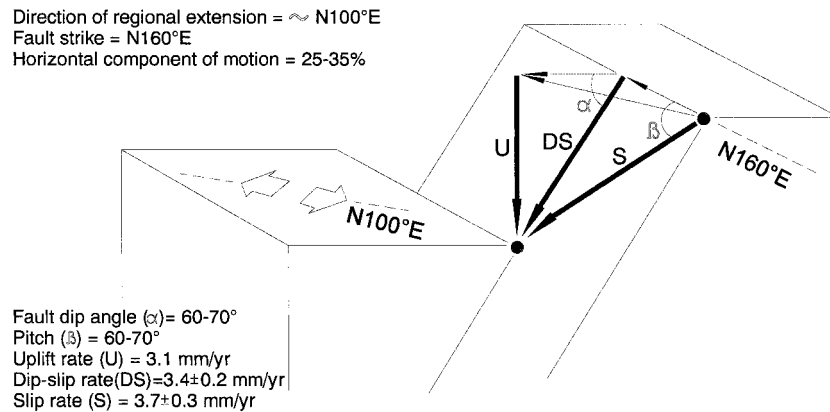
Direction of regional extension = ∿ N100°E
Fault strike = N160°E
Horizontal component of motion = 25-35%

Fault dip angle (α)= 60-70°
Pitch (β) = 60-70°
Uplift rate (U) = 3.1 mm/yr
Dip-slip rate(DS)=3.4±0.2 mm/yr
Slip rate (S) = 3.7±0.3 mm/yr

Figure 19. Block diagram showing western fault displacements with the various slip components.

4.2 January 11 event

The second and the main shock occurred at about 1.30 pm (GMT) and was catastrophic, devastating the entire south-eastern part of Sicily and killing about 54 000 people (Boccone 1697; Baratta 1901). Towns and villages located close to the southeastern coast of Sicily (Fig. 20b), such as Catania, Lentini, Carlentini, Augusta, Melilli, Floridia, Canicattini, Avola Antica and Noto Antica, which had already been seriously a ected by the event of January 9, were completely destroyed, su ering damage ascribed to an MCS intensity greater than X (Boschi *et al.* 1995a). Many other towns, located in an area extending from the eastern foot of Mt Etna to the southern coast of the Hyblean Plateau, such as Acireale, Palagonia, Militello, Vizzini, Buccheri, Giarratana, Ragusa, Modica, Scicli and Spaccaforno (present day Ispica), were extensively ruined, defining the area characterized by an MCS intensity of X (Boschi *et al.* 1995a).

The overall distribution of the e ects of the main shock shows, however, a few anomalies because of local seismic responses related to both geological and morphological conditions (Fig. 20b). Towns such as Occhiolà (present-day Grammichele), Mineo and Biscari (present-day Acate), located 10 km away from the mesoseismic area, were completely destroyed ($I = $ XI) because they were built on a thin layer of loose sands overlying clayey deposits. Conversely, the town of Siracusa, located within the mesoseismic area ($I > $ X), was a ected by damage ascribed to an MCS intensity of IX, as it was built on a large subhorizontal plateau made up of Tertiary carbonate rocks.

In order to better define the macroseismic picture of this event, a map showing the area including the towns and villages with a percentage of ruined buildings higher than 90 per cent (Table 2), derived from chronicle of Boccone (1697), and the e ects on the environment is shown in Fig. 20(c). The maximum ground-shaking region defines a 90 km long zone which, extending in a NE–SW direction along the coast, roughly corresponds to the area ascribed to an MCS intensity greater than X (Fig. 20c). The shock was particularly violent along the coast and it was dramatically felt in the towns of Catania, Augusta and Siracusa. In these localities (Boccone 1697; Bottone 1718; Baratta 1901) people were thrown in the air, massive floors and foundation stones were dislodged, and walls, together with their foundations, were shifted from their groundings, thus indicating a particularly strong vertical acceleration.

The main shock was felt as a roaring rumble in most of the towns located along the coast, and had considerable e ects on

the morphology (Fig. 20c). Large landslides occurred in several localities, for example Noto Antica, Sortino, Ferla, Cassaro and Spaccaforno (present-day Ispica). In the area located between Ferla and Cassaro (Boccone 1697; Bottone 1718), a massive rock-slide dammed a stream creating a lake with a circumference of about 3 miles (4.5 km) and a width of 250 paces (450 m). Near Sortino and Noto Antica, large landslides a ected the cultivated fields which, being located along the slopes of the major streams, slid for metres (Boccone 1697; Mongitore 1743).

The easternmost part of the mesoseismic area, between Catania and Noto Antica, was a ected by several linear fractures. The most impressive fractures, characterized by a length of about 250 paces (500 m) and a width of 8 spans (2 m) occurred in the plain south of Catania, 4 miles (6 km) onshore (Bottone 1718). Fractures and cracks were also recorded in Siracusa, Sortino, Melilli and Lentini (Boccone 1697).

Sand fountains spurted water to heights of several yards (up to 10 yards, corresponding to about 6–7 m), forming cones—mostly in the Lentini and Catania plains and along the valleys of the largest rivers (Boccone 1697; Bottone 1718).

The main shock also generated a large tsunami (Fig. 20c) recorded along the whole coast of eastern Sicily, between Messina and Siracusa, and on the island of Malta (Anonymous 1693; Boccone 1697; Bottone 1718; Baratta 1901). In the harbour of Catania, the sea retreated by several metres leaving boats stranded on the seafloor. When the sea returned, the wave, like '*a furious and rapid stream*' (Anonymous 1693), flung the boats beyond the walls, into the town. At Augusta and Siracusa (Boccone 1697; Bottone 1718) the sea retreated by 30 (60 m) and 50 (100 m) paces, respectively, then returned in a tidal wave which reached heights of 30 cubits (about 12 m). Galley ships of the Knights of Malta, anchored in the harbour of Augusta, ran aground on the seafloor because of the tidal waves (Baratta 1901). The tsunami was characterized by the occurrence of at least three distinct tidal waves which penetrated onland for about 50 paces (90–100 m) at Siracusa, 75 m at Augusta, where they lapped the walls of the monastery of San Domenico, about 250 m in Catania, where the sea reached the Piazza San Filippo (present Piazza Mazzini), and about 1 mile (1.5 km) at Mascali (Baratta 1901 and references therein).

Several aftershocks (Fig. 20d), felt in the villages and towns located close to the coastline extending between Catania and Siracusa, occurred up to 1696. The strongest shocks were
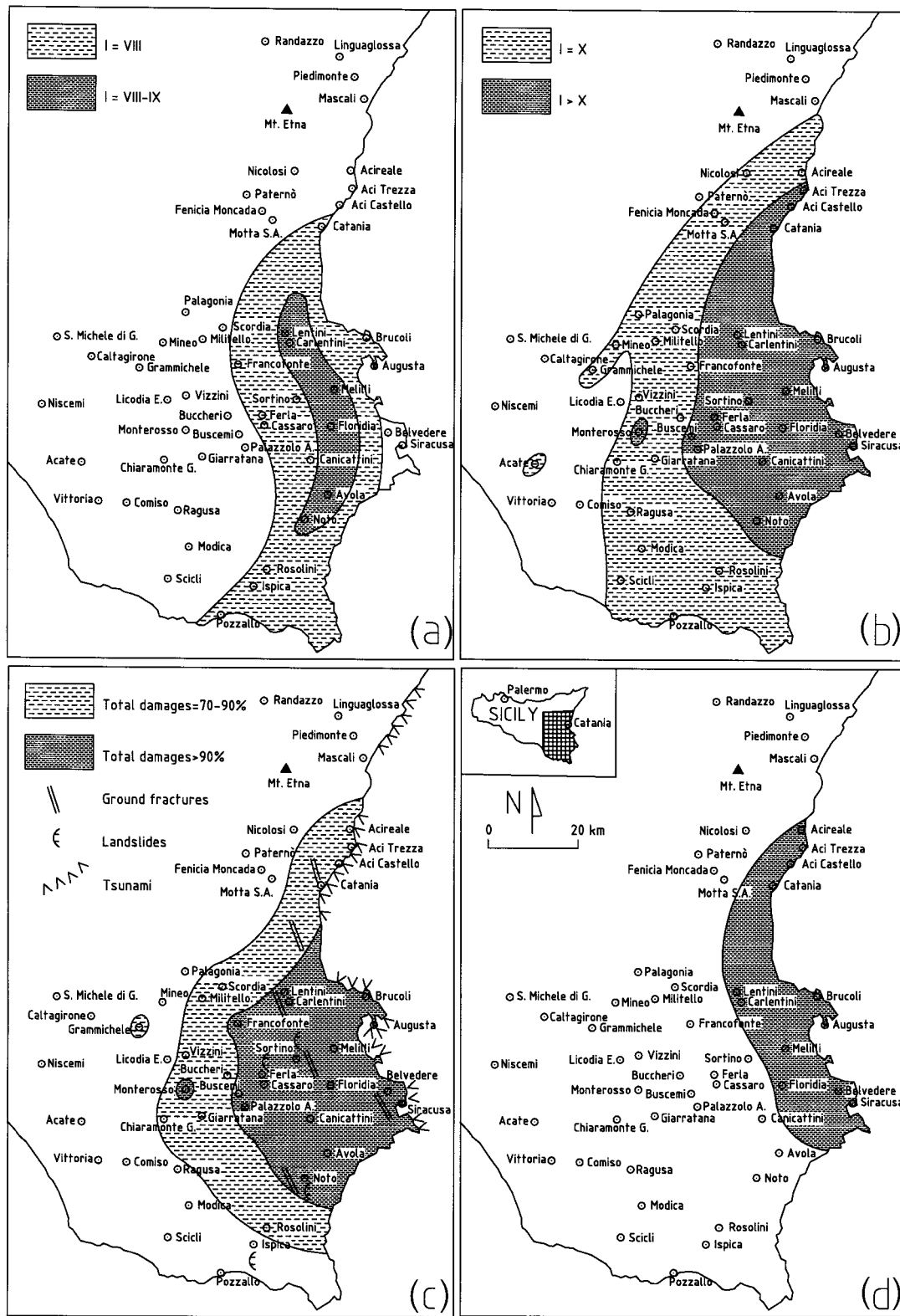
Figure 20. Cartoon showing the main features characterizing the 1693 January earthquakes. (a) Mesoseismic areas (MCS scale) related to the January 9 shock (data from Boschi *et al.* 1995a); (b) mesoseismic areas (MCS scale) related to the main shock of January 11 (data from Boschi *et al.* 1995a); (c) e ects on the environment and contour map of equal total damages of the main shock of January 11 based on data reported in Table 2 (data from Boccone 1697; Bottone 1718; Baratta 1901); (d) areas struck by 1693–1696 aftershocks (data from Boccone 1697; Bottone 1718; Mongitore 1743; Baratta 1901).

Table 2. Estimated devastation percentages for the 1693 January 11 earthquake. Descriptions of damage are from Boccone (1693).

Towns	Description of damage	Estimated percentage of devastation
Augusta	completely destroyed	100
Avola	completely destroyed and ruined	100
Buscemi	razed to the ground	100
Carlentini	completely destroyed	100
Cassaro	all in ruins	100
Ferla	totally devastated	100
Floridia	completely ruined	100
Francofonte	razed to the ground	100
Lentini	completely destroyed	100
Melilli	totally devastated	100
Mineo	completely destroyed	100
Monterosso	completely destroyed	100
Noto	completely destroyed	100
Occhiolà (Grammichele)	totally destroyed	100
Palazzolo	totally devastated	100
Sortino	completely destroyed	100
Siracusa	two parts of the town were totally devastated, the third part was severely damage	≈ 90
Acicastello	almost totally destroyed	≈ 90
Acireale	ruined, with less than a third of the houses left standing	> 70
Buccheri	devastated with few houses left standing	≈ 90
Catania	almost totally destroyed	≈ 90
Chiaramonte	destroyed, only few houses left standing	≈ 90
Giarratana	almost ruined with the castle partially damaged	≈ 90
Militello	only 300 houses were left standing	≈ 90
Scordia	two parts were devastated, the third part was damaged	≈ 70
Vizzini	two parts were totally ruined, the third part was uninhabitable	≈ 70
Caltagirone	half of the town was razed to the ground, a quarter was damaged	≈ 50
Comiso	very little damaged	< 50
Fenicia Moncada (Belpasso)	two third were in ruins	< 70
Licodia	many houses in ruins	< 50
Mascali	out of 300 houses, 140 were damaged and 35 did not su er any damage	< 50
Modica	half of the town destroyed	≈ 50
Niscemi	severely damaged	< 50
Palagonia	the fifth part was destroyed	≈ 20
Ragusa	almost two third destroyed	≤ 70
San Michele	only few houses were ruined	< 50
Scicli	mostly ruined with a few buildings left standing	> 70
Spaccaforno (Ispica)	severely damaged in the third part	< 50
Vittoria	only few houses were razed to the ground	< 50

recorded on 1693 April 1 and May 19, 1964 March 10, 1965 May 8 and September 23, and finally on 1696 April 20 (Boccone 1697; Bottone 1718; Mongitore 1743; Baratta 1901).

The above-mentioned observations produce a clear macroseismic picture of the two shocks of the 1693 January earthquakes. Damage related to the event of January 9 was significantly less severe than that which occurred during the main shock of January 11. The mesoseismic area was restricted to a narrow belt extending onshore from Lentini to Noto, thus suggesting that the epicentre of this shock was located along this belt, probably between Noto and Floridia. Conversely, the main shock of January 11 completely devastated the southeastern part of Sicily, producing dramatic environmental e ects. The coastal area was hit by a very large tsunami, and fractures, landslides and sand fountains occurred. Moreover, strong vertical ground accelerations a ected the coastal localities. This implies that the main shock of the 1693 events, which reached at least a magnitude of 7 (Westaway 1992), had an epicentre located o shore from the Ionian coast, not far from the coastline.

These features clearly indicate therefore that the two shocks had distinct epicentres: the first onland, probably along the Avola fault, one of the impressive normal faults that characterize the eastern margin of the Hyblean Plateau, and the second along the western fault located o shore along the Ionian coast between Catania and Siracusa.

5   DISCUSSION AND CONCLUSIONS

The data presented in this paper reveal the Quaternary extensional tectonics along the eastern border of the Hyblean Plateau in Sicily. This region is a ected by a prominent normal fault belt forming the southern edge of the Siculo–Calabrian rift zone (Monaco *et al.* 1997). Two trends of fault segments extend both onland and o shore, and strike NNW–SSE and NE–SW in the northern and southern parts of the study area, respectively.

Geological and morphological data suggest that the major activity of the NW–SE-trending normal fault segments of the Hyblean Plateau (e.g. Climiti, Mt Tauro, Thapsos, La

Maddalena faults) was earlier than ≈ 400 ka. In contrast, the activity on the NE–SW-striking segments of the Avola fault and Rosolini–Ispica fault system occurred between ≈ 400 ka and the present. Furthermore, seismic profiles indicate that the activity of NNW–SSW-trending major normal fault segments located in the Ionian oshore zone occurred between about 330 ka and the present. The length and depth distribution and extent of the synrift basins developed on the hanging walls of the Ionian oshore fault segments might suggest a more recent activity for the western fault (Fig. 13). Further evidence for the southwestern migration of fault activity is represented by the seafloor displacements recognizable along the western fault scarp.

The dating of the individual fault segments (marine and continental) aecting the eastern border of the Hyblean Plateau clearly indicates two sets of normal faults, which represent the response to dierent tectonic processes. The older NW–SE-trending normal faults, which bound the Lower–Middle Pleistocene small-sized basins of Augusta–Siracusa and Floridia, strike at normal angles to the main front of the Maghrebian thrust belt, thus representing extensional features developing in the foreland region in response to the NW–SE convergence between the Pelagian block and the orogenic belt. The younger fault segments, formed by normal faults in the Ionian oshore zone and by the Avola fault and the Rosolini–Ispica fault system, represent the active southern branch of the Siculo–Calabrian rift zone (Monaco *et al.* 1997) propagating southwards and cutting across the older collision-related extensional features.

The analysis of the historical chronicles that describe the January 1693 earthquakes clearly indicates two shocks with distinct epicentres located onland and oshore. We suggest that the 1693 January 9 seismic event can be attributed to the activity of the Avola fault, whereas the main shock of January 11 could be related to slip on the large western fault segment (about 45 km long) located oshore.

The statement that the events of 1693 January 9 and 11 are associated with two adjacent fault segments belonging to the same seismogenic zone could be in good agreement with changes of Coulomb failure stress caused by earthquake ruptures (Stein *et al.* 1992; King *et al.* 1994). In fact, according to this model, which has been tested for the fault segments in the Straits of Messina and in southern Calabria (Jacques *et al.* 1997), the rupture related to the shock of 1693 January 9 along the Avola fault induced changes in static stress on the neighbouring western oshore fault that could have triggered the subsequent main shock of January 11. Therefore, the western fault segment represents the most important fault, generating earthquakes with $M \sim 7$ in southeastern Sicily. Assuming a constant net slip rate of 3.7 ± 0.3 mm yr^{-1} and taking into account that earthquakes with $M \sim 7$ generated by normal faults give slips of 2–2.5 m (Wells & Coppersmith 1994), a recurrence interval of about 600 ± 100 yr might characterize earthquakes comparable to the main shock of the 1693 January 11.

To verify the reliability of these recurrence times, the earthquake history of southeastern Sicily has been briefly analysed. Earthquakes with features comparable to those characterizing the main shock of 1693 January 11 occurred in 122 and in 363 and 1169 (Mongitore 1743; Mercalli 1883; Baratta 1901; Caputo & Faita 1984; Boschi *et al.* 1995a). All these events, in fact, severely damaged the whole of eastern Sicily, generating large tsunamis recorded along the entire Ionian

coast of the island. We believe that they could be reasonably attributed to ruptures of the western fault in the Ionian oshore zone. Assuming that the occurrence of each earthquake of $M \sim 7$ represents the moment during which all the energy accumulated along the fault is completely relaxed, and that the recurrence time represents the period of the loading cycle between two consecutive seismic events, the periods between the historical earthquakes considered here are consistent with the proposed recurrence time of about 600 ± 100 years, except for the 1169 earthquake which, according to this scheme, occurred 806 years later than the event recorded in 363. This anomaly could be explained by variations of strength and/or loading rates along the master fault (Scholz 1990) or by the incompleteness of the earthquake catalogues for this historical period, which, being characterized by the barbarian and Arab invasions of Sicily, is documented only by rare and incomplete chronicles. Taking into account, however, that the time occurring between the 363 earthquake and the 1169 event is roughly twice the amount of the minimum value of the proposed recurrence time, the earthquake series could be completed by an earthquake that should have occurred during roughly the 8th century. Eectively, the chronicles report, even if with many uncertainties, the occurrence of two large earthquakes in eastern Sicily in 797 and in 853 (Bonito 1691; Mongitore 1743; Baratta 1901; Boschi *et al.* 1995a), which could fill the gap in the proposed earthquake series (Fig. 21).

To test this value of the recurrence time, the total number of earthquakes occurring along the western fault during the Holocene has been calculated using the seismic moment summation. Taking into account that the western fault, dipping at $60°–70°$, is about 45 km in length with earthquakes occurring
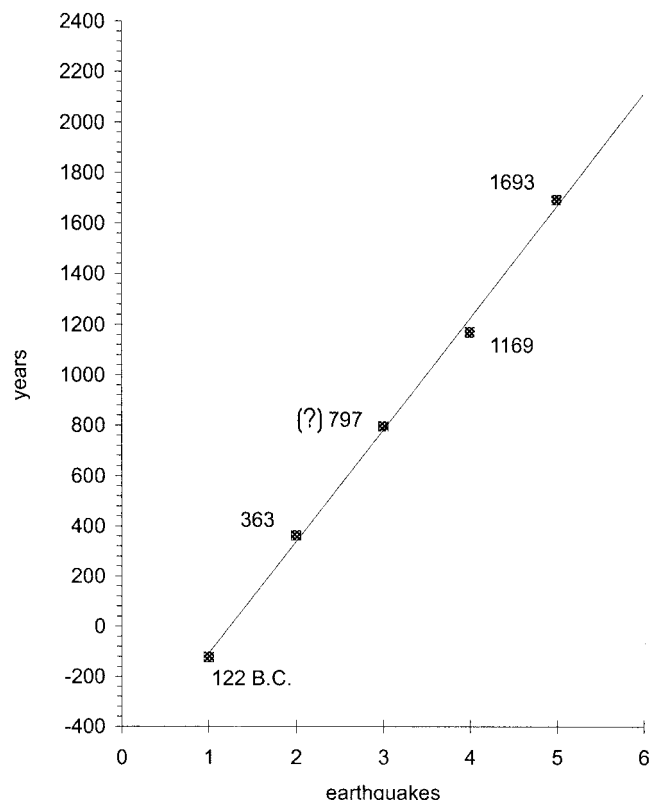

Figure 21. Time distribution of major earthquakes with MCS intensities greater than X occurring in southeastern Sicily.

at 10 km depth, the rupture area is about 540 km^2. Using a shear modulus of $\mu = 3.3 \times 10^{10}$ N m^{-2} and a displacement of 37 ± 3 m, a cumulative seismic moment of $M_0 = (6.5 \pm 0.5) \times 10^{20}$ N m for the last 10 kyr can be calculated. Given that the main shock with $M \sim 7$ on 1693 January 11 represents the characteristic earthquake occurring along the western fault, the associated seismic moment can be calculated with the relation $\log M_0 = 3/2(M + 6.03)$ of Hanks & Kanamori (1979), giving a value of $M_0 = 3.5 \times 10^{19}$ N m. This suggests that the Holocene displacement of the western fault could be the result of the total displacements related to 17–20 distinct earthquakes with $M \cong 7$, consistent with a recurrence time of about 550 ± 50 yr.

The main results of this study show that the Middle Pleistocene–Holocene deformation of southeastern Sicily is related to the activity of normal fault segments belonging to the southern edge of the Siculo–Calabrian rift zone (Tortorici *et al.* 1995; Monaco *et al.* 1997), which represents the most active seismic belt in the central Mediterranean, developing as a result of approximately ESE-striking extension. Morphological and geological information, together with the analysis of several seismic profiles carried out along the Ionian o shore zone, suggest that the most recent deformation of this region is related to the activity of three main fault segments represented onland by the NE–SW-striking Avola fault and the Rosolini–Ispica fault system and o shore by the NNW–SSE-trending western fault. The western fault represents one of the major fault segments of this area, with a length of about 45 km and a slip rate of 3.7 ± 0.3 mm yr^{-1}. On the basis of a detailed analysis of historical descriptions of the earthquake damage and e ects, we suggest that the seismic event of 1693 January 11, $M \sim 7$, could be related to rupture of the western fault. Finally, we propose a potential recurrence time of about 550 ± 50 yr for comparable large events on the western fault.

ACKNOWLEDGMENTS

REFERENCES

Accordi, B., 1963. Rapporti fra il Milazziano della costa iblea (Sicilia sud-orientale) e la comparsa di Elephas Mnaidriensis, *Geol. Romana,* **2,** 295–304.

Accordi, B., Campisi, B. & Colacicchi, R., 1959. Scoperta di un giacimento pleistocenico a elefanti nani e ghiro gigante nella grotta di Spinagallo (Siracusa), *Atti Acc. Gioenia Sci. Nat. Catania,* **12**(6), 167–181.

Alessio, M., Allegri, L., Antonioli, F., Belluomini, G., Ferranti, L., Improta, S., Manfra, L. & Proposito, A., 1992. Risultati preliminari relativi alla datazione di speleotemi sommersi nelle fasce costiere del Tirreno Centrale (Italy), *Giorn. di Geol.,* **54,** 165–193.

Anonymous, 1693. *Sincera ed esatta relazione dell'orribile terremoto seguito nell'Isola di Sicilia il di 11 di Gennaio 1693. Colla nota delle Città e Terre sprofondate, de'morti e luoghi che hanno patito, e con tutte le particolarità più degne da essere registrate,* Roma.

Antonioli, F. & Ferranti, L., 1996. La risalita del livello del Mare Tirreno nel corso dell'Olocene, Cinquanta anni di ricerche, *Mem. Soc. geol. It.,* **51,** 93–99.

Antonioli, F. & Frezzotti, M., 1989. I sedimenti tardo-pleistocenici ed olocenici compresi nella fascia costiera tra Sabaudia e Sperlonga, *Mem. Soc. geol. It.,* **41,** 321–334.

Armijo, R., Lyon-Caen, H. & Papanastassiou, D., 1991. A possible normal-fault rupture for the 464 Sparta earthquake, *Nature,* **351,** 137–139.

Armijo, R., Lyon-Caen, H. & Papanastassiou, D., 1992. East–west extension and Holocene normal-fault scarps in the Hellenic arc, *Geology,* **20,** 491–494.

Armijo, R., Meyer, B., King, G.C.P., Rigo, A. & Papanastassiou, D., 1996. Quaternary evolution of the Corinth Rift and its implications for the Late Cenozoic evolution of the Aegean, *Geophys. J. Int.,* **126,** 11–53.

Bada, J.L., Belluomini, G., Bonfiglio, L., Branca, M., Burgio, E. & Delitalia, L., 1991. Isoleucin epimerization ages of Quaternary mammals from Sicily, *Il Quaternario,* **4** (1a), 49–54.

Baratta, M., 1901. *I Terremoti d'Italia,* Arnaldo Forni, Bologna.

Basile, B. & Chilardi, S., 1996. *Siracusa—le Ossa Dei Giganti,* Arnaldo Lombardi, Siracusa.

Bassinot, F.C., Labeyrie, L.D., Vincent, E., Quidelleur, X., Shackleton, N.J. & Lancelot, Y., 1994. The astronomical theory of climate and the age of the Brunhes-Matuyama magnetic reversal, *Earth planet. Sci. Lett.,* **126,** 91–108.

Belluomini, G. & Bada, J.L., 1985. Isoleucine epimerization ages on the dwarf elephants of Sicily, *Geology,* **13,** 451–452.

Boccone, P., 1697. *Intorno al terremoto della Sicilia seguito l'anno 1693,* Museo di Fisica, Venezia.

Bonito, M., 1691. *Terra Tremante,* Arnaldo Forni, Bologna.

Bordonaro, S., Di Grande, A. & Raimondo, W., 1984. Lineamenti geomorfostratigrafici pleistocenici tra Melilli, Augusta e Lentini (Siracusa), *Boll. Acc. Gioienia Sci. Nat., Catania,* **17,** 65–88.

Bordoni, P. & Valensise, G., 1998. Deformation of the 125 ka marine terrace in Italy: tectonic implications, in *Coastal Tectonics,* pp. 71–110, eds Stewart, I.S. & Vita-Finzi, C., Geol. Soc. Lond. Spec. Publ., **146.**

Boschi, E., Ferrari, G., Gasperini, P., Guidoboni, E., Smriglio, G. & Valensise, G., 1995a. *Catalogo dei Forti Terremoti in Italia dal 461 a.c, al 1980,* Istituto Nazionale di Geofisica, S.G.A., Roma.

Boschi, E., Guidoboni, E. & Mariotti, D., 1995b. Seismic e ects of the strongest historical earthquakes in the Syracuse area, *Ann. Geofis.,* **38,** 223–253.

Bosi, C., Carobene, L. & Sposato, A., 1996. Il ruolo dell'eustatismo nella evoluzione geologica nell'area mediterranea, *Mem. Soc. geol. It.,* **51,** 363–382.

Bottone, D., 1718. *De immani Trinacriae traemotu, Idea historico-physica, in qua non solum telluris concussiones transactae recensetur, sed novissimae anni 1717,* Messina.

Brancaccio, L., 1968. Genesi e terrazzi delle forme costiere nella penisola sorrentina, *Boll. Soc. Natur. in Napoli,* **77,** 247–274.

Caputo, M. & Faita, G., 1984. Primo catalogo dei maremoti delle coste italiane, *Mem. Acc. Naz. Lincei,* **17,** 1–356.

Carbone, S., Cosentino, M., Grasso, M., Lentini, F., Lombardo, G. & Patanè, G., 1982. Elementi per una prima valutazione dei caratteri sismotettonici dell'Avampaese Ibleo (Sicilia sud-orientale), *Mem. Soc. geol. It.,* **24,** 507–520.

Cello, G., Guerra, I., Tortorici, L., Turco, E. & Scarpa, R., 1982. Geometry of the neotectonic stress field in southern Italy: geological and seismological evidence, *J. struct. Geol.,* **4,** 385–393.

Cernobori, L., Hirn, A., McBride, J., Nicolich, R., Petronio, L. & Romanelli, M., 1996. Crustal image of the Ionian basin and its Calabrian margins, *Tectonophysics,* **264,** 175–190.

Chappell, J. & Shackleton, N.J., 1986. Oxygen isotopes and sea level, *Nature,* **324,** 137–140.

Chappell, J., Omura, A., Esat, T., McCulloch, M., Pandolfi, J., Ota, Y. & Pillans, B., 1996. Reconciliation of late Quaternary sea levels derived from coral terraces at Huon Peninsula with deep sea oxygen isotope records, *Earth planet. Sci. Lett.,* **141,** 227–236.

Cogan, J., Rigo, L., Grasso, M. & Lerche, I., 1989. Flexural tectonics of southeastern Sicily, *J. Geodyn.,* **11,** 189–241.

Cosentino, D. & Gliozzi, E., 1988. Considerazioni sulle velocità di sollevamento di depositi eutirreniani dell'Italia meridionale e della Sicilia, *Mem. Soc. geol. It.,* **41,** 653–665.

D'Addezio, G. & Valensise, L., 1993. Metodologie per l'individuazione della struttura sismogenetica responsabile del terremoto del 13 dicembre 1990, in *Contributi allo Studio del Terremoto Della Sicilia Orientale del 13 Dicembre 1990,* pp. 115–125, eds Boschi, E. & Basili, A., Int. Report No 537, ING, Roma.

Dai Pra, G. & Hearty, P.J., 1989. Variazioni del livello del mare sulla costa ionica salentina durante l'Olocene, Epimerizzazione dell'Isoleucina in Helix sp, *Mem. Soc. geol. It.,* **42,** 311–320.

Dewey, J.F., Helman, M.L., Turco, E., Hutton, D.H.W. & Knott, S.D., 1989. Kinematics of the western Mediterranean, in *Alpine Tectonics,* pp. 265–283, eds Coward, M.P., Dietrich, D. & Park, R.G., Geol. Soc. Lond. Special Publ., **45.**

Di Grande, A. & Neri, M., 1988. Tirreniano a Strombus b. a M. Tauro (Augusta-Siracusa), *Rend. Soc. geol. It.,* **11,** 57–58.

Di Grande, A. & Raimondo, W., 1982. Linee di costa plio-pleistoceniche e schema litostratigrafico del Quaternario siracusano, *Geol. Romana,* **21,** 279–309.

Di Grande, A. & Scamarda, G., 1973. Segnalazione di livelli a Strombus bubonius LAMARCK nei dintorni di Augusta (Siracusa), *Boll. Acc. Gioienia. Sci. Nat., Catania,* **4,** 157–172.

Firth, C., Stewart, I., McGuire, W.J., Kershaw, S. & Vita-Finzi, C., 1996. Coastal elevation changes in eastern Sicily: implications for volcano instability at Mount Etna, in *Volcano Instability on the Earth and Other Planets,* pp. 153–167, eds McGuire, W.J., Jones, A.P. & Neuberg, J., Geol. Soc. Spec. Lond. Publ., **110.**

Gasparini, C., Iannacone, G., Scandone, P. & Scarpa, R., 1982. Seismotectonics of the Calabrian Arc, *Tectonophysics,* **82,** 267–286.

Gillot, P.Y., Kie er, G. & Romano, R., 1994. Evolution of Mt. Etna volcano in the light of potassium-argon dating, *Acta Vulcan.,* **5,** 81–87.

Grasso, M., De Dominicis, A. & Mazzoldi, G., 1990. Structures and tectonic setting of the western margin of the Hyblean–Malta shelf, Central Mediterranean, *Ann. Tecton.,* **4,** 140–154.

Grasso, M. & Lentini, F., 1982. Sedimentary and tectonic evolution of the eastern Hyblean Plateau (southeast Sicily) during Late Cretaceous to Quaternary times, *Palaeogeog. Palaeoclimat. Palaeoecol.,* **39,** 261–280.

Grasso, M. & Pedley, H.M., 1990. Neogene and Quaternary sedimentation patterns in the northwestern Hyblean Plateau (SE Sicily): the e ects of a collisional process on a foreland margin, *Riv. It. Palaeont. Stratigr.,* **96,** 219–240.

Hanks, T.C. & Kanamori, H., 1979. A moment–magnitude scale, *J. geophys. Res.,* **84,** 2348–2350.

Hirn, A., Nicolich, R., Gallart, J., Laigle, M., Cernobori, L. & ETNASEIS Scientific Group, 1997. Roots of Etna volcano in faults of great earthquakes, *Earth planet. Sci. Lett.,* **148,** 171–191.

Imbrie, J., Hays, J.D., Martinson, D.G., McIntyre, A., Mix, A.C., Morley, J.J., Pisias, N.G., Prell, W.L. & Shackleton, N.J., 1984. The orbital theory of Pleistocene climate: Support from a revised chronology of the marine ^{18}O record, in *Milankovitch and Climate,* Part 1, pp. 269–305, eds Berger, A., Imbrie, J., Hays, J., Kukla, G. & Saltzman, B. Plenum Reidel, Dordrecht.

Jacques, E., Monaco, C., Tapponnier, P., Benedetti, L. & Tortorici, L., 1997. Earthquakes triggering during the 1783 Calabria seismic sequence, *Abstract (Suppl. No. 1) Terra Nova,* **9,** 308.

Kie er, G., 1971. Dépots et niveaux marins et fluviatiles dé la region de Catane (Sicile), *Méditerranée,* **5–6,** 591–626.

King, G.C.P., Stein, R.S. & Lin, J., 1994. Static stress changes and the triggering of earthquakes, *Bull. seism. Soc. Am.,* **84,** 935–953.

King, G.C.P., Stein, R.S. & Rundle, J.B., 1988. The growth of geological structures by repeated earthquakes 1. Conceptual framework, *J. geophys. Res.,* **93,** 13 307–13 318.

Kusznir, N.J., Marsden, G. & Egan, S.S., 1991. A flexural-cantilever simple shear-pure shear model of continental lithosphere extension: applications to the Jeanne d'Arc Basin, Grand Banks and Viking Graben, North Sea, in *The Geometry of Normal Faults,* pp. 41–60, eds Roberts, A.M., Yielding, G. & Freeman, B., Geol. Soc. Lond. Spec. Publ., **56.**

Longaretti, G., Rocchi, S. & Ferrari, L., 1991. Il magmatismo dell'Avampaese Ibleo (Sicilia orientale) tra il Trias ed il Quaternario: dati di sottosuolo della Piana di Catania dal Pleistocene al Pliocene, *Mem. Soc. geol. It.,* **47,** 537–556.

Makris, J., Nicolich, R. & Weigel, W., 1986. A seismic study in the western Ionian Sea, *Ann. Geophys.,* **6,** 665–678.

Malatesta, A., 1985. *Geologia e Palaeobiologia dell'era Glaciale,* La Nuova Italia Scientifica, Roma.

Martinson, D.G., Pisias, N.G., Hays, J.D., Imbrie, J., Moore, T.C. Jr & Shackleton, N.J., 1987. Age dating and the orbital theory of ice ages: development of a high-resolution 0–300 000 years chronostratigraphy, *Quat. Res.,* **27,** 1–29.

Mastronuzzi, G., Palmentola, G. & Ricchetti, G., 1989. Aspetti della evoluzione olocenica della costa pugliese, *Mem. Soc. geol. It.,* **42,** 287–300.

Mazzuoli, R., Tortorici, L. & Ventura, G., 1995. Oblique rifting in Salina, Lipari and Vulcano islands (Aeolian Islands, Southern Italy), *Terra Nova,* **7,** 444–452.

Mercalli, G., 1883. *Vulcani e Fenomeni Vulcanici in Italia,* Arnaldo Forni, Bologna.

Merritts, D. & Bull., W.B., 1989. Interpreting Quaternary uplift rates at the Mendocino triple junction, northern California, from uplifted marine terraces, *Geology,* **17,** 1020–1024.

Michetti, A.M., Brunamonte, F., Serva, L. & Vittori, E., 1996. Trench investigations of the 1915 Fucino earthquake fault scarps (Abruzzo, central Italy): Geological evidence of large historical events, *J. geophys. Res.,* **101,** 5921–5936.

Monaco, C., 1997. Tettonica pleistocenica nell'area a sud dell'Etna (Sicilia orientale), *Il Quaternario,* **10**(2)**,** 393–398.

Monaco, C., Petronio, L. & Romanelli, M., 1995. Tettonica estensionale nel settore orientale del Monte Etna (Sicilia): dati morfotettonici e sismici, *Studi Geologici Camerti,* Volume Speciale, **2,** 363–374.

Monaco, C., Tapponnier, P., Tortorici, L. & Gillot, P.Y., 1997. Late Quaternary slip rates on the Acireale-Piedimonte normal faults and tectonic origin of Mt. Etna (Sicily), *Earth planet. Sci. Lett.,* **147,** 125–139.

Monaco, C. & Tortorici, L., 1995. Tettonica estensionale quaternaria nell'Arco Calabro e in Sicilia orientale, *Studi Geologici Camerti,* Volume Speciale, **2,** 351–362.

Mongitore, A., 1743. Istoria cronologica de' terremoti in Sicilia, in *Della Sicilia Ricercata Nelle Cose Più Memorabili,* Vol. 2, pp. 345–445, Palermo.

Mulargia, F., Broccio, F., Achilli, V. & Baldi, P., 1985. Evaluation of a seismic quiescence pattern in southeastern Sicily, *Tectonophysics,* **116,** 335–364.

Piatanesi, A. & Tinti, S., 1998. A revision of the eastern Sicily earthquake and tsunami, *J. geophys. Res.,* **103,** 2749–2758.

Piccardi, L., Gaudemer, Y., Tapponnier, P. & Boccaletti, M., 1999. Active oblique extension in the central Apennines (Italy): evidence from the Fucino region, *Geophys. J. Int.,* **139,** 499–530 (this issue).

Pirazzoli, P.A., Mastronuzzi, G., Saliège, J.F. & Sansò, P., 1997. Late Holocene emergence in Calabria, Italy, *Mar. Geol.,* **141,** 61–70.

Postpischl, D., 1985a. *Catalogo dei Terremoti Italiani Dall'anno 1000 al 1980,* CNR, Progetto Finalizzato Geodinamica, Graficoop, Bologna.

Postpischl, D., 1985b. *Atlas of Isoseismal Maps of Italian Earthquakes,* CNR, Progetto Finalizzato Geodinamica, Graficoop, Bologna.

Rhodes, E.J., 1996. ESR dating of tooth enamel, in *Siracusa—le Ossa dei Giganti,* pp. 39–44, eds Basile, B. & Chilardi, S., Arnaldo Lombardi, Siracusa.

Roberts, A.M. & Yielding, G., 1991. Deformation around basin-margin faults in the North Sea/mid-Norway rift, in *The Geometry of Normal Faults,* pp. 61–78, eds Roberts, A.M., Yielding, G. & Freeman, B., Geol. Soc. Lond. Spec. Publ., **56.**

Sartori, R., Colalongo, M.L., Gabbianelli, G., Bonazzi, C., Carbone, S., Curzi, P.V., Evangelisti, D., Grasso, M., Lentini, F., Rossi, S. & Selli, L., 1991. Note stratigrafiche e tettoniche sul rise di Messina (Ionio nord-occidentale), *Giorn. di Geol.,* **53,** 49–64.

Scandone, P., Patacca, E., Radoicic, R., Ryan, W.B.F., Cita, M.B., Rawson, M., Chezar, H., Miller, E., Mckenzie, J. & Rossi, S., 1981. Mesozoic and Cenozoic rocks from Malta Escarpment (Central Mediterranean), *Am. Assoc. Petrol. Geol. Bull.,* **65,** 1299–1319.

Scholz, C.H., 1990. *The Mechanics of Earthquakes and Faulting,* Cambridge Universiy Press, Cambridge.

Shackleton, N.J. & Opdyke, N.D., 1973. Oxygen isotope and palaeo-magnetic stratigraphy of Equatorial Pacific core V28–238: Oxygen isotope temperature and ice volumes on a 105 year and 106 year time scale, *Quat. Res.,* **3,** 39–55.

Stein, R.S., King, G.C.P. & Rundle, J.B., 1988. The growth of geological structures by repeated earthquakes 2. Field examples of continental dip-slip faults, *J. geophys. Res.,* **93,** 13 319–13 331.

Stein, R.S., King, G.C.P. & Lin, J., 1992. Change in failure stress on the southern San Andreas fault system caused by the 1992 magnitude = 7.4 Landers earthquake, *Science,* **258,** 1328–1332.

Stewart, I., Cundy, A., Kershaw, S. & Firth, C., 1997. Holocene coastal uplift in the Taormina area, northeastern Sicily: implications for the southern prolongation of the Calabrian seismogenic belt, *J. Geodyn.,* **24,** 37–50.

Stewart, I. & Hancock, P.L., 1991. Scales of structural heterogeneity within neotectonic normal fault zones in the Aegean region, *J. struct. Geol.,* **13,** 191–204.

Tapponnier, P., Armijo, R., Manighetti, I. & Courtillot, V., 1990. Bookshelf faulting and horizontal block rotations between over-lapping rifts in southern Afar, *Geophys. Res. Lett.,* **17,** 1–4.

Tortorici, L., Monaco, C., Tansi, C. & Cocina, O., 1995. Recent and active tectonics in the Calabrian arc (Southern Italy), *Tectonophysics,* **243,** 37–55.

Ward, S.N., 1994. Constraints on the seismotectonics of the central Mediterranean from Very Long Baseline Interferometry, *Geophys. J. Int.,* **117,** 441–452.

Wells, D.L. & Coppersmith, K.J., 1994. New empirical relationships among magnitude, rupture, length, rupture width, rupture area and surface displacement, *Bull. seism. Soc. Am.,* **84,** 974–1002.

Westaway, R., 1992. Seismic moment summation for historical earthquakes in Italy: tectonic implications, *J. geophys. Res.,* **97,** 15 437–15 464.

Westaway, R., 1993. Quaternary uplift of southern Italy, *J. geophys. Res.,* **98,** 21 741–21 772.